2001-03

Digital LPI Radar Detector

Ong, Peng Ghee; Teng, Haw Kiad

Monterey, California: Naval Postgraduate School.

http://hdl.handle.net/10945/43859

NAVAL POSTGRADUATE SCHOOL
Monterey, California

THESIS

DIGITAL LPI RADAR DETECTOR

by

Ong, Peng Ghee
Teng, Haw Kiad

March 2001

Thesis Advisor: D. C. Schleher
Second Reader: D. C. Jenn

Approved for public release; distribution is unlimited

REPORT DOCUMENTATION PAGE			Form Approved OMB No. 0704-0188
Public reporting burden for this collection of information is estimated to average 1 hour per response, including the time for reviewing instruction, searching existing data sources, gathering and maintaining the data needed, and completing and reviewing the collection of information. Send comments regarding this burden estimate or any other aspect of this collection of information, including suggestions for reducing this burden, to Washington headquarters Services, Directorate for Information Operations and Reports, 1215 Jefferson Davis Highway, Suite 1204, Arlington, VA 22202-4302, and to the Office of Management and Budget, Paperwork Reduction Project (0704-0188) Washington DC 20503.			
1. AGENCY USE ONLY *(Leave blank)*	**2. REPORT DATE** March 2001	**3. REPORT TYPE AND DATES COVERED** Master's Thesis	
4. TITLE AND SUBTITLE: Title (Mix case letters) Digital LPI Radar Detector			**5. FUNDING NUMBERS**
6. AUTHOR(S) Peng Ghee Ong, Haw Kiad Teng			
7. PERFORMING ORGANIZATION NAME(S) AND ADDRESS(ES) Naval Postgraduate School Monterey, CA 93943-5000			**8. PERFORMING ORGANIZATION REPORT NUMBER**
9. SPONSORING / MONITORING AGENCY NAME(S) AND ADDRESS(ES) N/A			**10. SPONSORING / MONITORING AGENCY REPORT NUMBER**
11. SUPPLEMENTARY NOTES The views expressed in this thesis are those of the author and do not reflect the official policy or position of the Department of Defense or the U.S. Government.			
12a. DISTRIBUTION / AVAILABILITY STATEMENT Approved for public release; distribution is unlimited			**12b. DISTRIBUTION CODE**

13. ABSTRACT ***(maximum 200 words)***

The function of a Low Probability of Intercept (LPI) radar is to prevent its interception by an Electronic Support (ES) receiver. This objective is generally achieved through the use of a radar waveform that is mismatched to those waveforms for which an ES receiver is tuned. This allows the radar to achieve a processing gain, with respect to the ES receiver, that is equal to the time-bandwidth product of the radar waveform. This processing gain allows the LPI radar to overcome the range-squared advantage of the ES receiver in conventional situations. Consequently, a conventional ES receiver can only detect an LPI radar at very short ranges (<3 nm).

The focus of this thesis was to develop an ES receiver to detect LPI radar signals with the same sensitivity as conventional pulse signals. It implements a detector which employs a technique, known as "deramping," that forms an adaptive matched filter to the linear FMCW LPI radar signal in order to achieve the processing gain that is equal to the received signal's time-bandwidth product. An experimental transmitter was built to emulate the radar signal with FMCW characteristics and transmitted through a standard gain horn. The transmitted signal is then received via a receiver horn, mixed down to an intermediate frequency (IF), sampled by an A/D convertor and digitally deramped using a Pentium II computer.

It was demonstrated that the LPI radar signal can be extracted from the noise background by means of digital deramping.

14. SUBJECT TERMS FMCW, LPI, LPI radar, deramp, PILOT, chirp, frequency-modulated continuous wave			**15. NUMBER OF PAGES**
			16. PRICE CODE
17. SECURITY CLASSIFICATION OF REPORT Unclassified	**18. SECURITY CLASSIFICATION OF THIS PAGE** Unclassified	**19. SECURITY CLASSIFICATION OF ABSTRACT** Unclassified	**20. LIMITATION OF ABSTRACT** UL

NSN 7540-01-280-5500

Standard Form 298 (Rev. 2-89)
Prescribed by ANSI Std. 239-18

THIS PAGE INTENTIONALLY LEFT BLANK

Approved for public release; distribution is unlimited

DIGITAL LPI RADAR DETECTOR

Peng Ghee Ong
Maj, Republic of Singapore Air Force
B.E., Nanyang Technological Institute, 1992

Haw Kiad Teng
Maj, Republic of Singapore Navy
B.S.E.E., U. S. Coast Guard Academy, 1992

Submitted in partial fulfillment of the
requirements for the degree of

MASTER OF SCIENCE IN SYSTEMS ENGINEERING

from the

NAVAL POSTGRADUATE SCHOOL
March 2001

Author: _____
Peng Ghee Ong

_____
Haw Kiad Teng

Approved by: _____
Curtis Schleher, Thesis Advisor

_____
Dave Jenn, Second Reader

_____
Dan Boger, Chairman
Information Warfare Academic Group

THIS PAGE INTENTIONALLY LEFT BLANK

ABSTRACT

The function of a Low Probability of Intercept (LPI) radar is to prevent its interception by an Electronic Support (ES) receiver. This objective is generally achieved through the use of a radar waveform that is mismatched to those waveforms for which an ES receiver is tuned. This allows the radar to achieve a processing gain, with respect to the ES receiver, that is equal to the time-bandwidth product of the radar waveform. This processing gain allows the LPI radar to overcome the range-squared advantage of the ES receiver in conventional situations. Consequently, a conventional ES receiver can only detect an LPI radar at very short ranges (<3 nm).

The focus of this thesis was to develop an ES receiver to detect LPI radar signals with the same sensitivity as conventional pulse signals. It implements a detector which employs a technique, known as "deramping," that forms an adaptive matched filter to the linear FMCW LPI radar signal in order to achieve the processing gain that is equal to the received signal's time-bandwidth product. An experimental transmitter was built to emulate the radar signal with FMCW characteristics and transmitted through a standard gain horn. The transmitted signal is then received via a receiver horn, mixed down to an intermediate frequency (IF), sampled by an A/D convertor and digitally deramped using a Pentium II computer.

It was demonstrated that the LPI radar signal can be extracted from the noise background by means of digital deramping.

THIS PAGE INTENTIONALLY LEFT BLANK

TABLE OF CONTENTS

I. INTRODUCTION 1
A. BACKGROUND 1
1. Radar Vulnerability 1
2. LPI Radar 1
3. ES Receiver 2
B. THESIS OBJECTIVES 3
1. Adaptive Digital Matched Filter Design 3
C. PERFORMANCE VERIFICATION 4
D. THESIS ORGANIZATION 4

II. THEORY OF LPI RADAR DETECTION 5
A. LPI RADAR WAVEFORM AND PERFORMANCE 5
1. Linear FMCW Waveform 5
2. Instantaneous Frequency 6
3. LPI Radar Ranging and Resolution 7
4. Processing Gain 10
B. THE LPI PILOT RADAR 10
C. LPI RADAR DETECTOR 11
1. Adaptive Matched Filter for LPI Radar Detection 12
D. DIGITAL LPI RADAR DETECTOR 17
1. Components of a Digital LPI Radar Detector 19
2. Selection of Intermediate Frequency (IF) 19
3. Digital Deramping 20
E. LPI RADAR DETECTION IN PULSE RADAR ENVIROMENT 21

III. HARDWARE 23
A. HARDWARE SETUP 23
B. TRANSMITTER 25
1. Voltage Controlled Oscillator (VCO) Transceiver 25
2. Function Generator 26
3. Variable Attenuator 27
4. Antennas 28
C. RECEIVER 29
1. Directional Coupler 29
2. Low-Noise Amplifier 30
3. Bandpass Filter (RF Selection) 31
4. Mixer and Local Oscillator 32
5. Video Amplifier 33
6. Bandpass Filter (IF Selection) 33
D. OTHER HARDWARE REQUIRED 34
1. Power Supplies 34
2. Cables and Connectors 35
E. OVERALL SYSTEM GAIN CONSIDERATIONS 35

IV. SOFTWARE 39
A. COMPUSCOPE 2125 39
1. Sampling Rate 39
2. Dynamic Range 40
B. MATLAB CODE 41
1. Signal Capturing 41
2. Deramping Channels 43
3. Digital Deramping 43
4. Power Spectral Density 44
5. Digital Low Pass Filter 44
6. Thresholding 46
7. Hit Counting 47
a. Threshold-crossing blocks are 2 or less 47
b. Block with less than 25% of channel's chirp bandwidth 47
8. Channel Selection 47

V. RESULTS AND ANALYSIS 49
A. MODE DETERMINATION 49
1. Matched Signal 49
2. Chirp Bandwidth Mismatch 51
3. No Signal 52
4. Pulse Radar 53
B. UNSYNCHRONIZED SIGNALS 54
C. DETECTION 56
1. Weak Signals 56
2. Detection Capability 57

VI. CONCLUSIONS AND RECOMMENDATIONS 59
A. CONCLUSIONS 59
B. RECOMMENDATIONS 59

LIST OF REFERENCES 61

APPENDICES 63
A. DERAMPING SOFTWARE (MATLAB CODE) 63
B. DATA CAPTURING CODE (MATLAB CODE) 66
C. PARAMETER SETTING FOR THE COMPUSCOPE 2125 A/D CARD (MATLAB CODE) 67
D. OTHER MODE DETECTION RESULTS 68
1. Table of Summary for Results Enclosed 68

INITIAL DISTRIBUTION LIST 81

LIST OF FIGURES

Figure 2.1 Linear-FMCW Transmitted and Received Signals 7
Figure 2.2 Output Spectrum of a Completely Deramped Signal 13
Figure 2.3 Output Spectrum of a Deramped Signal with a Frequency not Equal to the Carrier Frequency 14
Figure 2.4 Output Spectrum of a Deramped Signal with Phase Offset 15
Figure 2.5 LPI Radar Detector Block Diagram 16
Figure 2.6 Digital LPI Radar Detector Block Diagram 18
Figure 2.7 No Harmonic Distortion 20
Figure 2.8 Harmonic Distortion 20
Figure 2.9 Masking of Conventional Pulsed Radar Signal 21
Figure 3.1 Hardware Setup Block Diagram 23
Figure 3.2 Transmitter Setup 24
Figure 3.3 Receiver Setup 24
Figure 3.4 MA-COM MA87728-M01 Voltage Control Oscillator 25
Figure 3.5 Hewlett-Packard Model-3314A Function Generator 26
Figure 3.6 Tektronix 2465B oscilloscope 26
Figure 3.7 HP X375A Variable Attenuator 27
Figure 3.8 HP8495B variable attenuator 27
Figure 3.9 Transmitter Standard Gain Horn 28
Figure 3.10 Receiver Standard Gain Horn 28
Figure 3.11 Omni-Spectra model 50056-30 Directional Coupler with Attenuator 29
Figure 3.12 HP8566B Spectrum Analyzer 30
Figure 3.13 MITEQ Low Noise Amplifier 30
Figure 3.14 TTE Model-K3910-9.375G-SMA Bandpass Filter 31
Figure 3.15 MITEQ DM-0812-LW2 Mixer 32
Figure 3.16 Gigatronics Model-600 Microwave Signal Generator 32
Figure 3.17 MITEQ Model-AU-1291 Video Amplifier 33
Figure 3.18 4B120-76/50-0 Bandpass Filter 33
Figure 3.19 HP6114A Precision Power Supply 34
Figure 3.20 HP Model-6216A Power Supply 34
Figure 3.21 Noise Figure Block Diagram 35
Figure 4.1 MATLAB Program Flow Chart 42
Figure 4.2 Chirp Bandwidth of Deramping Channels 43
Figure 4.3 PSD of Deramped Signal (before LPF) 44
Figure 4.4 Frequency Response of Digital Lowpass Filters 45
Figure 4.5 PSD of Deramped output after LPF 45
Figure 4.6 Example of Thresholding 46
Figure 5.1 Deramped Output of a 1.5625 MHz Bandwidth FMCW Signal 49
Figure 5.2 Deramped Output of a 50 MHz Bandwidth FMCW Signal 50
Figure 5.3 Deramped Output of a 30 MHz Bandwidth FMCW Signal 51
Figure 5.4 Deramped Ouput of a 40 MHz Bandwidth FMCW Signal 51
Figure 5.5 Deramped Output of Noise-Only Signal 52

Figure 5.6 Deramped Output of a Pulse Radar 53
Figure 5.7 Deramped Output of 50MHz FMCW (a) Synchronized (b) Unsynchronized 54
Figure 5.8 Deramped Output of 50MHz FMCW Shifted in Steps of 10% of Pulse Duration 55
Figure 5.9 Deramped Output of Weak Signals 56

LIST OF TABLES

Table 2.1 PILOT Radar Technical Specifications 11
Table 2.2 PILOT Radar Performance 11
Table 4.1 Maximum Power and Resolution of CompuScope 2125 40
Table 5.1 LPI Receiver Detection Ranges 57
Table 5.2 Theoretical and Practical System Sensitivity 58

THIS PAGE INTENTIONALLY LEFT BLANK

ACKNOWLEDGMENTS

I would like express my gratitude to the followings without whom this thesis would not have been possible; Professor D. C. Schleher for providing the initial idea for this thesis, continued guidance and advice; My wife, and our three children, Lucas, Lucinda and Luisa for their regular source of joy, support and encouragement throughout the process of thesis preparation; Paul Buczynski and Dave Schaeffer for their relentless assistance in rendering hardware support for the experiment.

Maj Ong Peng Ghee

I would like to thank the professors, faculty and staff at the Naval Postgraduate School who imparted to me their valuable knowledge and experience during my study here. In particular, I thank Prof Schleher for all his guidance in helping us complete this thesis.

Abel and Elliot, thanks for tearing me away from the computer to take a break when I needed to. I also thank my wife for her love, care and support without which I can never complete my course here. Jia Shuan, I love you.

Finally, and most of all, I thank God for His grace in providing in ways far beyond I can imagine or ask for. Thank you, Jesus.

Maj Teng Haw Kiad

THIS PAGE INTENTIONALLY LEFT BLANK

I. INTRODUCTION

A. BACKGROUND

1. Radar Vulnerability

Conventional design of radars requires that the transmitted microwave signal be sent out in pulses so that the duration between transmission and reception can be measured to determine the range of the target. However, this form of transmission also requires a substantial peak power making them vulnerable to detection by relatively modest intercept receivers. In military applications, these interceptions can be exploited by the enemy to implement Electronic Attack in the form of Anti-Radiation Missiles (ARM) or jamming. The need to deny interception leads to the development of Low Probability of Intercept (LPI) radars.

2. LPI Radar

One of the techniques used in the LPI radars in an attempt to escape detection is the use of a wideband, high-duty cycle transmitter waveform to spread the radiated energy over a wide spectrum of frequencies. The ES receiver must process a large bandwidth in search of the LPI radar of interest thus accepting an equivalent band of noise. The LPI radar is thus able to exploit the time-bandwidth product by reducing its peak transmitted power to bury itself in the environmental noise. Due to this mismatch in waveforms for which the ES receiver is tuned, the LPI radar is effectively invisible to the ES receiver.

Presently, LPI radars are used in covert operations by ships and submarines, as well as for coastal and battlefield surveillance. Forecast International has predicted the use of such radars for silent targeting by Anti-ship Cruise Missiles (ASCM), and anti-submarine warfare periscope detection [3].

3. ES Receiver

With the widespread use of FMCW type LPI radars, it becomes critical for current ES systems to detect these radars in order to fulfill its operational function. Most existing ES receivers operate on the basis of a single signal sample and have little or no capability to detect internal signal modulation such as that employed in the FMCW radar. However, if the FMCW signal characteristic is known to the ES receiver, it is then possible to synthesize a matched filter for the specific FMCW waveform. The technique employed, known as "deramping," is discussed in later parts of this thesis. With the use of a matched filter, the ES receiver regains the range advantage (the one-way vis-à-vis round trip transmission for the radar) as it will also be able to achieve the processing gain that is equal to the time-bandwidth product of the LPI radar signal.

B. THESIS OBJECTIVES

The focus of this thesis is to develop an ES receiver to detect LPI radar signals with the same sensitivity as conventional pulse signals. It is the objective of this thesis to implement a detector which employs a technique, known as "deramping," that forms an adaptive matched filter to the linear FMCW LPI radar signal in order to achieve the processing gain that is equal to the received signal's time-bandwidth product.

An experimental transmitter was built to emulate the LPI radar signal with FMCW characteristics and radiate it through a standard gain horn. The transmitted signal is then received via a receiver horn, mixed down to an intermediate frequency (IF), sampled by an A/D converter and digitally deramped using MATLAB residing in a Pentium II computer. Details of the setup are covered in Chapter II.

1. Adaptive Digital Matched Filter Design

The original intention was to carry out the deramping process in analog form. However, for various reasons that will be covered in Chapter II, it was decided that the digital process is more efficient. Since the deramping is carried out digitally, it also became necessary for the signal to be sampled at an intermediate frequency in order that the band of interest remains within the sampling capability of the A/D converter. Moreover, the amount of data to be processed is significantly reduced.

The digital deramping process allows for a larger number of deramping channels that is limited only by the processing capability of the CPU instead of hardware in the case of analog deramping. The deramping channels' parameters are digitally set to match the target radar's characteristics. The number of channels and bandwidth of each channel can easily be changed as the program is written in MATLAB. This adds tremendous amount of flexibility in setting and configuration changes.

The receiver can detect the presence of a FMCW radar if its chirp bandwidth within the band of interest set in the receiver. If the parameters are set accurately, the receiver can also determine the mode of operation of the target LPI radar.

C. PERFORMANCE VERIFICATION

The Philips Indetectable Low Output Transceiver (PILOT) radar is chosen as the target radar to verify the performance of the Digital LPI Radar Receiver. The known modes of operation of the radar consist of 6 different sweep frequencies, namely, 50 MHz, 25 MHz, 12.5 MHz, 6.25 MHz, 3.125 MHz, and 1.5625 MHz. These sweep bandwidths are set as the 6 deramping channels in the performance verification. It is demonstrated that the presence of the PILOT radar in each of the 6 modes can be detected and identified.

D. THESIS ORGANIZATION

Technical aspects of the LPI Radar and the Digital LPI Receiver are covered in Chapter II. It also explains the development and design considerations for the receiver.

The Digital LPI Receiver comprises two main parts: the hardware and the software subsystems. The hardware setup for both the transmitter and receiver is covered in Chapter III while the MATLAB software design of the matched filter is discussed in Chapter IV.

Chapter V, compiles the results obtained to provide the system capabilities and limitations. An analysis of the results is also included in this chapter.

Finally, conclusions and recommendations are summarized in Chapter VI.

II. THEORY OF LPI RADAR DETECTION

LPI radar utilizes the spread spectrum technique to generate sufficient processing gain to achieve low-level signal detection capability. Hence, unlike the conventional radar signal which has high signal-to-noise ratio, the LPI radar signal is deeply buried in the background noise (SNR $\leq$ - 40dB). In contrast with communication system, it is difficult to completely isolate LPI radar signal to determine its features. To add to the complexity, the LPI radar signal is further imbedded in field of conventional radar pulses with much greater peak powers (up to 60dB higher than LPI radar signal).

In theory, LPI radar uses random noise-like waveforms to produce a thumbtack-type ambiguity function [4, 5]. However, such waveforms do not generally perform well for radar operations, especially detecting target with background clutter. Practical LPI radars generally have more definite waveform structures which are more susceptible to detection. The wideband linear FM-CW type signal, employed in the PILOT/SCOUT radar system, is a common waveform structure used to achieve LPI operation [1, 6, 7].

A. LPI RADAR WAVEFORM AND PERFORMANCE

1. Linear FMCW Waveform

Being the most extensively used pulse compression waveform for radar application, the linear FMCW signal naturally becomes the target of study in this thesis. The operating principle of a Linear FMCW radar is best understood by examining its characteristics; namely the transmitted (carrier) frequency, the slope of the FM and the repetition period. These features are clearly visualized by examining the expression for a general FM-CW signal

$$v(t) = A\, e^{j\left(2\pi f_c t + \frac{\pi f_s t^2}{T}\right)} \tag{2.1}$$

A = *signal amplitude*

f_c = *carrier frequency*

f_s = *FM sweep deviation*

T = *repetition period*

$\frac{f_s}{T}$ = *FM (chirp) slope*

2. Instantaneous Frequency

In the time domain, the instantaneous frequency, f_i, of the above signal can be obtained by differentiating the part in the parenthesis of Equation 2.1,

$$\begin{aligned} 2\pi f_i &= \frac{d}{dt}\left(2\pi f_c t + \frac{\pi f_s t^2}{T}\right) \\ &= 2\pi f_c + \frac{2\pi f_s t}{T} \\ &= 2\pi f_c + 2\pi\alpha t \end{aligned} \tag{2.2}$$

$\alpha = \frac{f_s}{T}$ *is the FM slope*

Equation 2.2 clearly demonstrates the linear relationship of the instantaneous frequency with time. The frequency against time plot of a FM-CW signal is as thus shown in Figure 2.1. A Linear FMCW signal can thus be generated by modulating a carrier with a sawtooth input.

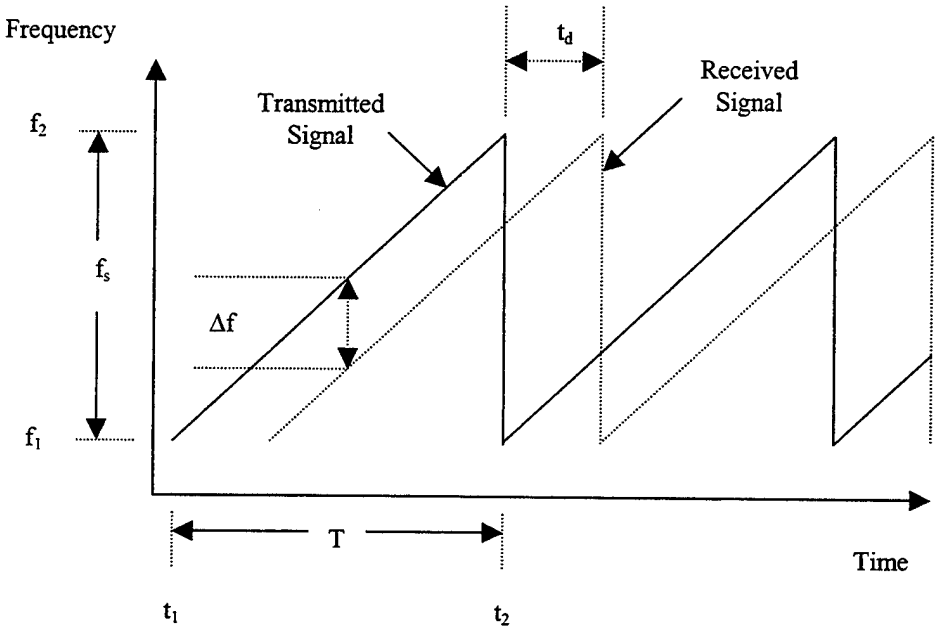

Figure 2.1 Linear-FMCW Transmitted and Received Signals

3. LPI Radar Ranging and Resolution

To determine the range of a target, the linear-FMCW radar mixes the signal reflected from the target with a portion of the transmitted signal to generate a 'beat' frequency (Δf) which is the difference between the 2 frequencies. The mixer's output, *y(t)*, is given as

$$\begin{aligned} y(t) &= A_t e^{j\left(2\pi f_c t + \frac{\pi f_s t^2}{T}\right)} \times A_r e^{-j\left[2\pi f_c (t-t_d) + \frac{\pi f_s (t-t_d)^2}{T}\right]} \\ &= A_t A_r e^{j\left[2\pi f_s t_d + \frac{2\pi f_s t_d t}{T} + \frac{\pi f_s t_d^2}{T}\right]} \end{aligned} \tag{2.3}$$

As before, the instantaneous frequency of the mixer output is determined by the differentiating the part in parenthesis in Equation 2.3

$$2\pi\Delta f = \frac{d}{dt}\left(\frac{2\pi f_s t_d t}{T}\right)$$

$$= \frac{2\pi f_s t_d}{T}$$

$$\Delta f = \frac{f_s}{T} t_d = \frac{f_s}{T}\frac{2R}{c} \tag{2.4}$$

$$R = \frac{\Delta f\, T\, c}{2 f_s} \tag{2.5}$$

R = range of the target

Δf = 'beat' frequency

c = velocity of propagation

Equation 2.4 indicates that the 'beat' frequency (Δf) is proportional to the time delay (t_d) between the transmitted and received signal, which is proportional to the range R of the target.

Under a normal operating environment, the FM-CW radar will generally receive many signals from targets at different ranges simultaneously. These signals will combine to form a complex waveform at the output of the receiver mixer. The complex waveform, after A/D conversion, is resolved into its frequency components using the Fast Fourier Transform (FFT). The width of each frequency bin of the FFT process represents a range increment and the amplitude of that bin is the echo strength of the target at that range. The output of the FFT is normally further processed and converted into a 'regular' analog video signal which is suitable for PPI display or used for tracking purposes.

For any radar waveform, the ideal range resolution, ΔR, is linearly proportional to time resolution, ΔT, and inversely proportional to the bandwidth of the transmitted waveform, BW, as given below:

$$\Delta R = \frac{c\,\Delta T}{2} = \frac{c}{2\,BW} \tag{2.6}$$

ΔR = *range resolution*

ΔT = *time resolution*

BW = *the signal bandwidth*

For example, a 50MHz FM sweep deviation (bandwidth) corresponds to time resolution no less than 2ns and a range resolution of

$$\Delta R = \frac{c}{2\,BW} = \frac{\left(3\times10^{8}\right)}{2\times\left(50\times10^{6}\right)} = 3\,m \tag{2.7}$$

A lower sweep deviation of 1.5625 MHz will yield a poorer range resolution of

$$\Delta R = \frac{c}{2BW} = \frac{\left(3\times10^{8}\right)}{2\times\left(1.5625\times10^{6}\right)} = 96\,m \tag{2.8}$$

Since range resolution is dependent on the bandwidth of the system, changing the features of the chirp signal can therefore vary it. The higher the FM sweep deviation of FM-CW radar, the better the resolution of the system.

Unfortunately, high resolution obtained from large FM sweep deviation comes with a price. The trade-off for the better range resolution is a decrease in the maximum unambiguous range of the radar. The maximum unambiguous range is limited by the size and number of range cells (frequency bins) of the FFT process. For example, a 512-point FFT processor, employed by the PILOT/SCOUT radar systems, produces 512 range cells. For a 50MHz FM sweep deviation, the maximum unambiguous range, R_u, is less than one nautical mile. Conversely, 1.5625MHz FM sweep deviation will result in a much longer range (26.5nm)

$$R_u = 512\,cells \times \frac{3\,m}{cell} = \frac{1536}{1852}nm = 0.83\,nm \tag{2.9}$$

$$R_u = 512\,cells \times \frac{96\,m}{cell} = \frac{49152}{1852}nm = 26.5\,nm \tag{2.10}$$

To achieve longer range, a FM-CW radar must sweep a shorter frequency span and thus sacrifice range resolution. The trade-off between unambiguous range and range resolution leads to the radar having to operate with various modes: higher resolution modes at shorter ranges and lower resolution modes at longer ranges.

4. Processing Gain

Processing gain of a linear FM-CW radar stems from the fact that the radar can integrate the returns coherently over the whole sweep period (T) producing an effective noise bandwidth equal to 1/T Hz. The PILOT/SCOUT radar system, having a sweep period of 1ms, accomplished an effective noise bandwidth of 1 kHz. Based on a minimum and maximum sweep deviations of 1.5625 and 50 MHz respectively, it can achieve a processing gain of approximately 32 to 47 dB

$$G_p\,(dB) = 10 \times \log\left(\frac{1.5625 \times 10^6}{1000}\right) = 31.9\ dB \tag{2.11}$$

$$G_p\,(dB) = 10 \times \log\left(\frac{50 \times 10^6}{1000}\right) = 47.0\ dB \tag{2.12}$$

Typical intercept receivers are designed to detect pulsed or simple CW signals and are unable to capitalize on the processing gain to seek out low-level FM-CW radar signal. The processing gain of the FM-CW radar allows it to detect a signal of much lower power (on the order equal to the processing gain) than conventional pulse radar, and that gives it its LPI capability.

B. THE LPI PILOT RADAR

As the subject of this experiment, the linear FM-CW signal structure is further investigated by examining the manner in which it is implemented in the PILOT LPI Radar. The PILOT radar features will be used as a yardstick to evaluate the effectiveness of the proposed Digital LPI Radar Detector.

The PILOT utilizes the above described wideband linear FM-CW principle to transmit a chirp signal at a center frequency of 9.345 to 9.405 GHz. Table 2.1 lists the pertinent technical specifications of the PILOT radar. Based on Equations 2.6, 2.9 and 2.11, the processing gains, range resolutions and maximum unambiguous ranges for the modes of operation (for various frequency sweep) are tabulated in Table 2.2.

Parameters	Specifications
Antenna Type	Single or dual slotted waveguide
Antenna Gain	30 dB
Antenna Sidelobes	< -40 dB
Beamwidth (3 dB)	1.2° azimuth, 20° elevation
Polarization	Horizontal
Scan Rate	24 rpm
Output Power	1W, 100mW, 10mW, 1mW
Frequency	9.345 – 9.405 MHz
Frequency Sweep	50, 25, 12.5, 6.25, 3.125, 1.5625 MHz
Sweep Repetition Frequency	1 kHz
Instrumented Range	0.75, 1.5, 3, 6, 12, 24 n miles
Receiver Noise Figure	3 dB
Number of Range Cells	512

Table 2.1 PILOT Radar Technical Specifications

Frequency Sweep (MHz)	Processing Gain (dB)	Range Resolution (m)	Unambiguous Range (n miles)
1.5626	47	96	26.54
3.125	44	48	12.27
6.25	41	24	6.63
12.5	38	12	3.32
25	35	6	1.65
50	32	3	0.83

Table 2.2 PILOT Radar Performance

With a frequency sweep of 50 MHz and a repetition frequency of 1 kHz, the PILOT radar yields a processing gain of 47 dB. An intercept receiver will have a disadvantage of 23.5 dB (224-to-1) reduction in intercept range (to about 2 – 3 nm) when attempting to detect the PILOT radar signal.

C. LPI RADAR DETECTOR

In order that an ELINT interceptor can extract the LPI signal from the noise background, it must first have an adaptive matched filter that has the capability to tune to

the possible features of the LPI radar waveform. Next, it has to discern any spurious signals caused by non-LPI radars operating within the same environment.

1. Adaptive Matched Filter for LPI Radar Detection

To detect LPI radar signal at operationally useful ranges, the intercept receiver must overcome the processing gain disadvantage. The only way to regain the processing gain is to form a matched filter to the LPI radar waveform. Achieving similar processing gain, the interceptor's signal detection capability will be identical to that of the LPI radar; that is, dependent only on the energy contained within the signal. This will then permit the extraction of LPI radar signal from a noise background. If the adaptive filter is faithfully matched with the LPI waveform, instead of being disadvantaged, the interceptor now has a 23.5 dB advantage over the LPI radar.

To construct a faithful matched filter, the transmitted frequency, the slope of the FM and the repetition period, have to be known. However, these features of interest are not normally known to the LPI radar interceptor. As such, the matched filter has to be adaptively formed. The LPI radar signals have to be estimated and incorporated into the matched filter and adaptively changed as part of the detection process. In the construction of the adaptive matched filter, any inaccuracy in the feature estimates (mismatched filter) will lead to a loss in processing gain. The loss in processing gain due to a mismatched filter can be derived using the radar ambiguity function [4,5]. In turn, the intercept receiver's range can be determined.

An adaptive matched filter for the PILOT radar waveform was developed using a technique employed by pulse compression radar, called deramping [1]. The deramping process mixes the input signal with a locally generated linear FM signal to produce an output signal of reduced FM slope in comparison with the input signal, as demonstrated by Equations 2.13 to 2.15:

$$y(t) = v(t) \times s(t) \tag{2.13}$$

$y(t)$ = *mixer output of LPI Intercepter*
$v(t)$ = *received LPI signal*
$s(t)$ = *locally generated deramping signal*

$$\begin{aligned} y(t) &= A_t e^{j(2\pi f_c t + \pi \alpha t^2)} \times A_r e^{j(2\pi f_l t + \pi \alpha_1 t^2)} \\ &= A_t A_r e^{j[2\pi (f_c - f_l)t + 2(\alpha - \alpha_l)t^2]} \end{aligned} \tag{2.14}$$

The instantaneous frequency of Equation 2.14 is as follows:

$$2\pi f_i = 2\pi (f_c - f_l) + 2\pi (\alpha - \alpha_1)t \tag{2.15}$$

$$FM\ slope = \alpha - \alpha_1 \qquad (reduced\ FM\ slope)$$

When the output signal FM slope is reduced to zero there is only a d.c. component present, and the signal is completely deramped. When this happens, a matched filter for the input waveform is faithfully constructed. For complete deramping, the locally generated center frequency, f_l, and FM slope, α_1, are identical to the input signal, f_c, and FM slope, α, respectively. The output will contain only a d.c. component; i.e., the FM slope is zero

$$\begin{aligned} y(t) &= A_t e^{j\left(2\pi f_c t + \frac{\pi f_s t^2}{T}\right)} \times A_r e^{-j\left[2\pi f_c t + \frac{\pi f_s t^2}{T}\right]} \\ &= A_t A_r \qquad (d.c.component\ only) \end{aligned} \tag{2.16}$$

The spectrum is depicted in Figure 2.2.

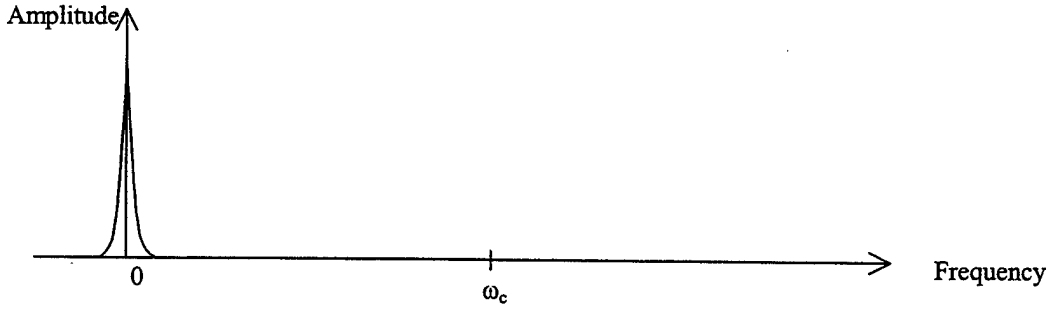

Figure 2.2 Output Spectrum of a Completely Deramped Signal

If the carrier frequency of the matched filter differs from that of the input signal, then a single tone single output whose frequency results that is the difference between the two signals ($f_c - f_l$). However, if f_l is zero, only the carrier frequency will be present at the output

$$\begin{aligned} y(t) &= A_t e^{j\left(2\pi f_c t + \frac{\pi f_s t^2}{T}\right)} \times A_r e^{-j\left[2\pi f_l t + \frac{\pi f_s t^2}{T}\right]} \\ &= A_t A_r e^{j[2\pi(f_s - f_l)t]} \\ &\text{if } f_l = 0, \\ y(t) &= A_t A_r e^{j2\pi f_c t} \qquad (\textit{carrier frequency only}) \end{aligned} \tag{2.17}$$

This is depicted in Figure 2.3.

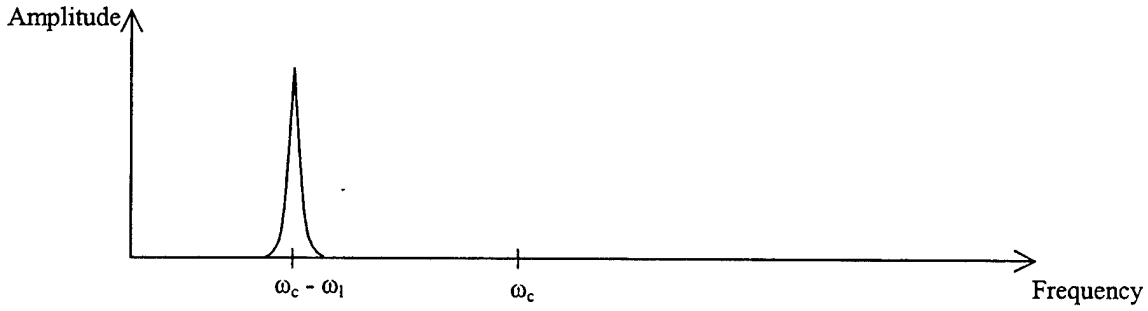

Figure 2.3 Output Spectrum of a Deramped Signal with a Frequency not Equal to the Carrier Frequency

If there is a de-synchronization in the phase between the input signal and the matched filter, two single-tone signals will be produced

$$\begin{aligned} v(t) &= A_t e^{j\{[2\pi f_c - 2\pi\alpha(T-t_0)]t + \pi\alpha t^2\}}\left[u(t) - u(t-t_0)\right] \\ &+ A_t e^{j\{2\pi f_c(t-t_0) + \pi\alpha(t-t_0)\}}\left[u(t-t_0) - u(t-T)\right] \end{aligned} \tag{2.18}$$

$$\begin{aligned} y(t) &= v(t) \times s(t) \\ &= A_t A_r e^{j[2\pi f_c + 2\alpha t_0]t}\left[u(t) - u(t-t_0)\right] \\ &+ A_t A_r e^{j[(2\pi f_c - 2\alpha t_0)t + t_0(\alpha t_0 - 2\pi f_c)]}\left[u(t-t_0) - u(t-T)\right] \end{aligned} \tag{2.19}$$

The frequency separation between the 2 single-tone signals will be equal to the FM sweep deviation of the chirp signal.

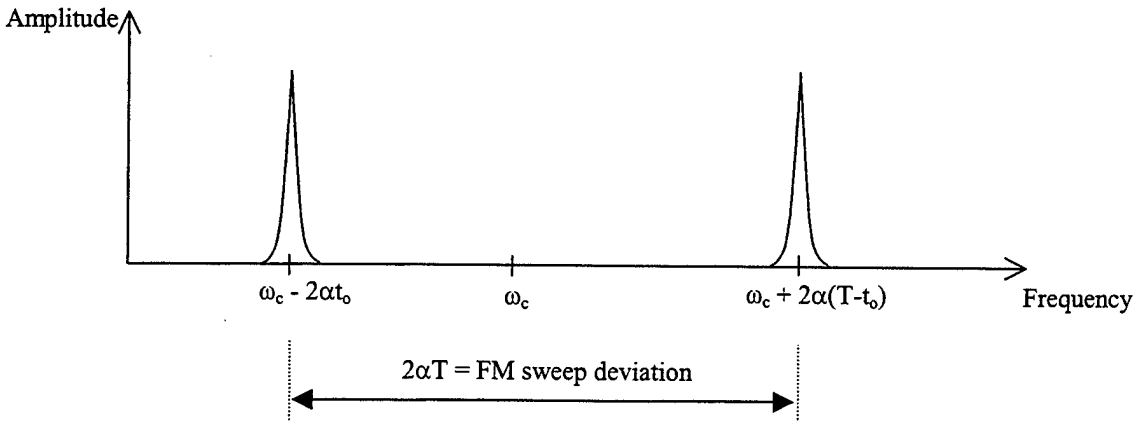

Figure 2.4 Output Spectrum of a Deramped Signal with Phase Offset

From the analysis of the deramping process, the frequency range of the output can be predicted when the features of the matched filter are closely tuned to that of the target LPI Radar waveform. The output of the deramped signal can then be easily processed using a FFT filter bank that covers the expected frequency range. Figure 2.5 shows an example of a LPI radar detector using analog deramping [7].

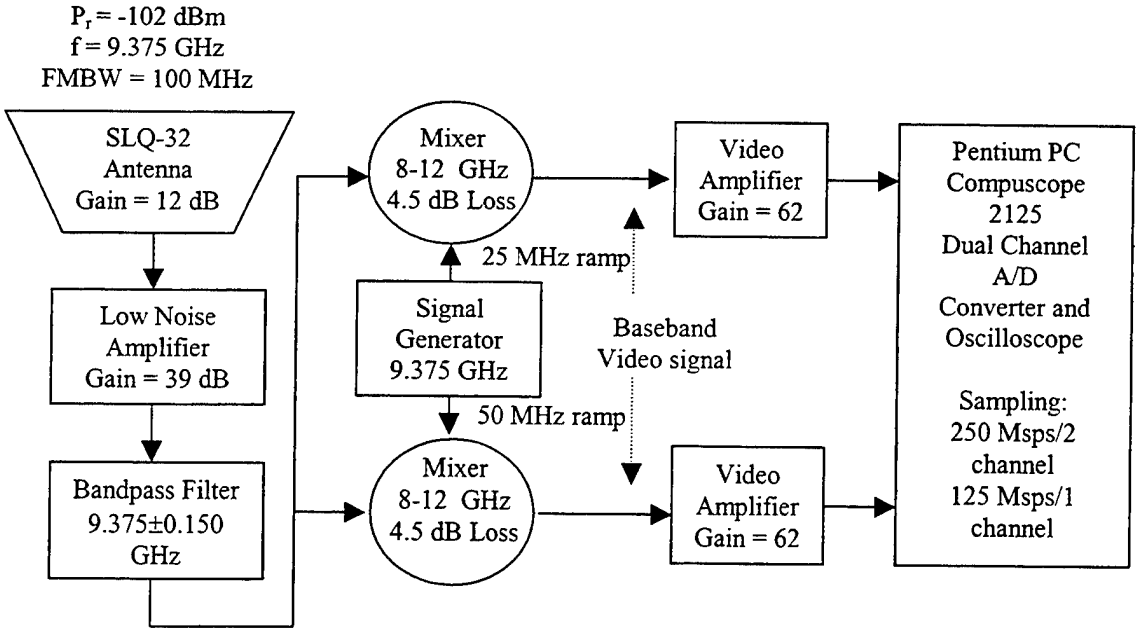

Figure 2.5 LPI Radar Detector Block Diagram

Besides facilitating the determination of the frequency content, the output frequency spectrum (FFT output) can also be observed to assess the faithfulness of the matched filter. If two widely separated FFT filters, a wide band of filters or a combination are energized, the features of the matched filter have to be re-tuned to synchronize it to the LPI signal. A re-adjustment of the FM repetitive frequency or the phase of the matched filter or both may be necessary.

The LPI radar detector shown in Figure 2.5 consists of two analog deramping channels that allow the bandwidth of the LPI radar to be estimated and the mode of operation inferred. However, the two-channel analog system is more likely to result in mismatched conditions that lead to larger losses in processing gain and ultimately reduction detection range. Upon possible detection, any filter re-tuning will have to be done through intricate analog electronics. To overcome this, a Digital LPI Radar Detector was proposed for the experiment.

D. DIGITAL LPI RADAR DETECTOR

The matched filter of a Digital LPI Radar Detector is software generated. Deramping of the LPI radar signal is achieved through digital signal processing. This provides flexibility in signal processing as the features of the matched filter can be re-tuned with ease using the software algorithm. Another merit of digital deramping is that the input signal need not be continuously present during the detection process. In contrast, analog deramping requires the input to be present at all time during the mixing and re-tuning process. In this aspect, the digital system requires only a period of the incoming signal to be captured (1 ms for PILOT radar). Once digitally captured, the input signal can be manipulated using software. Deramping and matched filter re-tuning can be done using the already captured signal or any processed version of it. This makes software generated matched filter truly adaptive. A block diagram of the Digital LPI Radar Detector is depicted in Figure 2.6

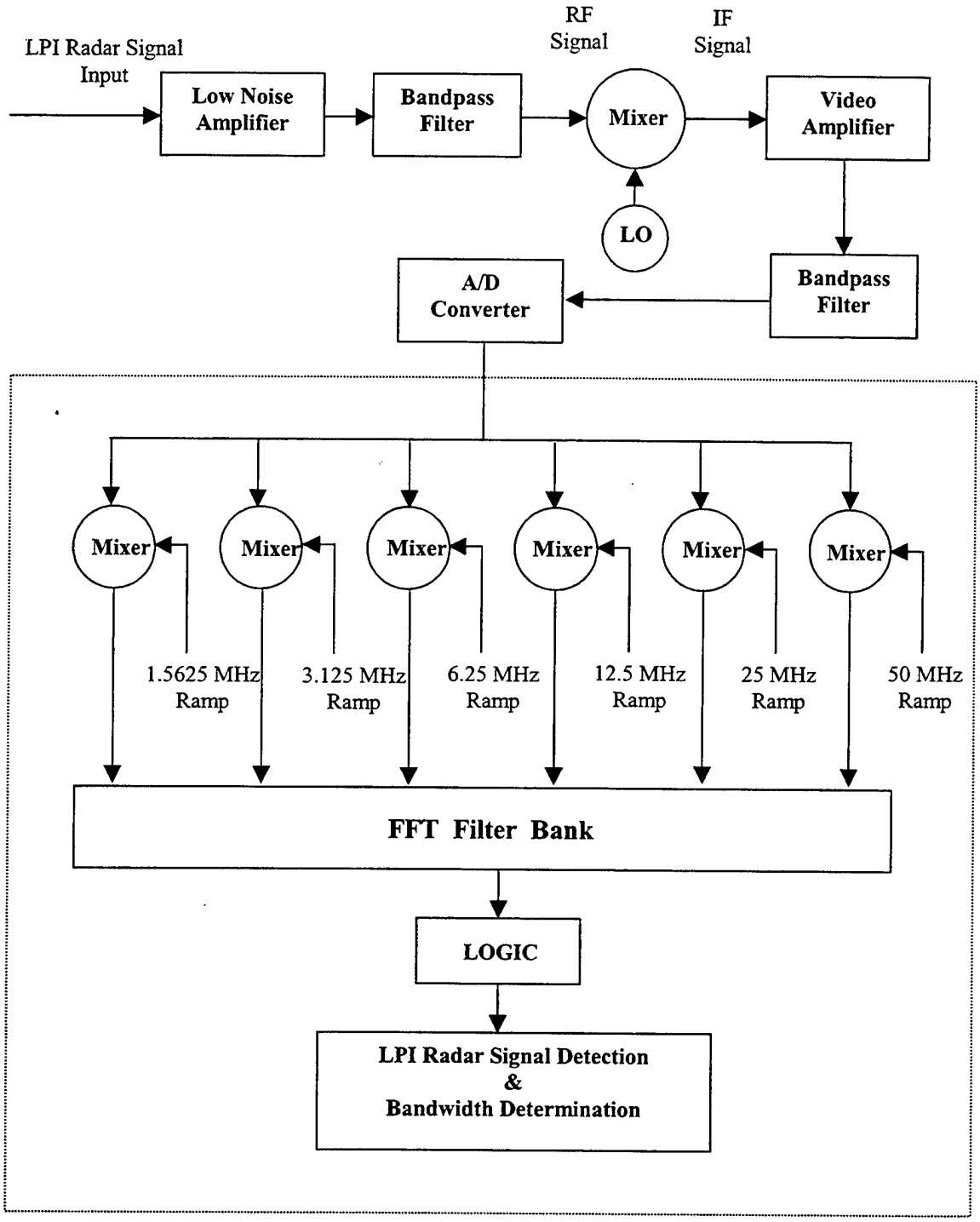

Figure 2.6 Digital LPI Radar Detector Block Diagram

1. Components of a Digital LPI Radar Detector

A low noise amplifier (LNA), with high gain and low noise figure, is placed at the front of the detector to improved the overall system noise figure. The first bandpass filter serves as the RF channel selector. The incoming RF signal is converted into an IF signal through heterodyning. The conversion of RF to IF signal is essential to reduce the amount of digital data needed to capture the input signal. For Nyquist sampling, the RF signal will require many giga-bytes of data for a 1 ms long signal while only kilobytes are required for IF. Before A/D conversion, the IF signal is boosted to a level within the dynamic range of the Analog-to-Digital Convertor (ADC) using a video amplifier.

The amplified IF signal is then sampled at above Nyquist Rate to avoid aliasing. The noise allowed into the system is limited by a IF bandpass filter. The noise level is reduce to a minimum by selecting the BPF bandwidth equal to that of the chirp bandwidth. A Data Acquisition Board converts and captures the IF signal digitally. Only one period of the signal is required for the digital deramping process. The final component of the Digital LPI Radar Detector is the software deramping algorithm.

2. Selection of Intermediate Frequency (IF)

If the IF is set too high, the sampling rate has to be increased correspondingly to prevent aliasing during the ADC and DAC process. Setting it too low will introduce harmonic distortion. The second harmonic generated during the heterodyne process will interfere with the original signal if they are not sufficiently spaced. The minimum IF should be at least 1.5 times that of the highest frequency sweep expected. For example, a 75 MHz IF is needed for a 50 MHz chirp signal to avoid harmonic distortion (see Figure 2.7).

$$
\begin{aligned}
IF &= 75\ MHz \\
Freq\ \ Band\ \ 1 &= 50\ -100\ MHz \\
2nd\ \ Harmonic &= 150\ MHz \\
Freq\ \ Band\ \ 2 &= 100\ -\ 200\ MHz
\end{aligned}
\tag{2.20}
$$

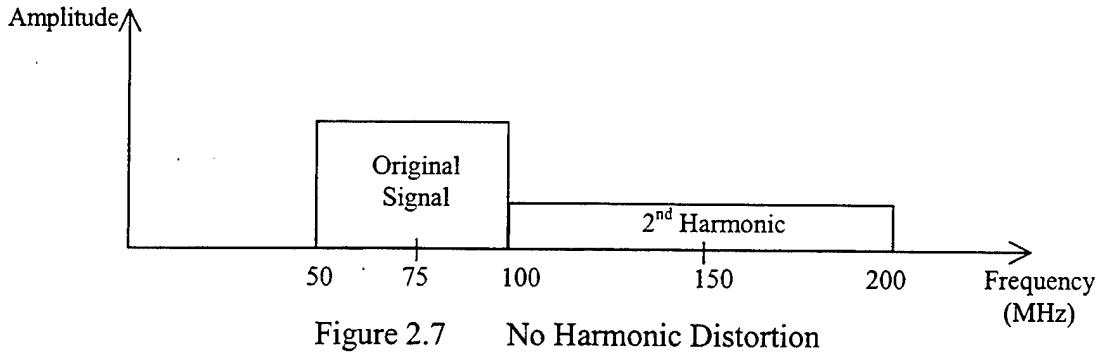

Figure 2.7 No Harmonic Distortion

When the IF is below 75 MHz, say 60 MHz, harmonic distortion will occur as depicted in Figure 2.8.

$$
\begin{aligned}
IF &= 60\ MHz \\
Freq\ \ Band\ \ 1 &= 35\ -85\ MHz \\
2nd\ \ Harmonic &= 120\ MHz \\
Freq\ \ Band\ \ 2 &= 70\ -170\ MHz
\end{aligned}
\tag{2.21}
$$

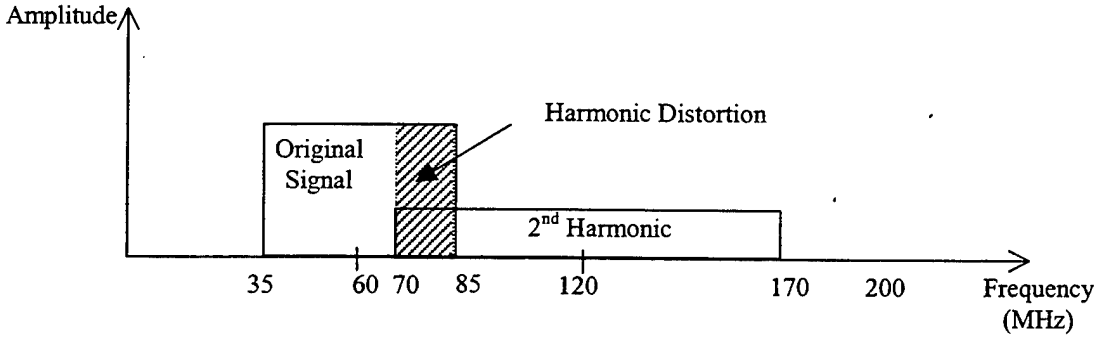

Figure 2.8 Harmonic Distortion

3. Digital Deramping

Six software generated matched filters are used to deramp the captured signal digitally. The filters are designed to match the six operating modes of the PILOT radar. The 6-channel arrangement reduces the degree of mismatch to achieve sufficient

processing gain for initial detection. Detection is determined by examining the output of a FFT filter bank using a constant false alarm rate (CFAR) scheme that sets the threshold for determining the channel hit. The channel that yields an initial detection can have its features adaptively changed (using the software algorithm) to fine-tune its matched filter to achieve optimal processing gain

Although the above Digital LPI Radar Detector is tailored to the PILOT radar, it can be easily adapted to detect other LPI radar. A library of threat radar can be digitally stored and incorporated whenever needed, based on intelligence assessment. In the event that the LPI radar is not one which can be found in the library, experimental results in Chapter 5 demonstrated that the system is still capable of detecting mismatched linear FMCW signals at operationally useful ranges.

E. LPI RADAR DETECTION IN PULSE RADAR ENVIROMENT

The simplicity of the proposed Digital LPI Radar Detector allows it to be piggy-backed onto an existing Electronic Intelligence (ELINT) or ES receiver. When the operating environment is flooded with pulsed radar signals where peak powers are up to 60 dB higher, the LPI radar detector can be over-whelmed and cease to function as designed. In this case, a temporal mask, shown in Figure 2.9, can be used to eliminate the conventional pulsed signals before the input is investigated for the present of LPI radar signal.

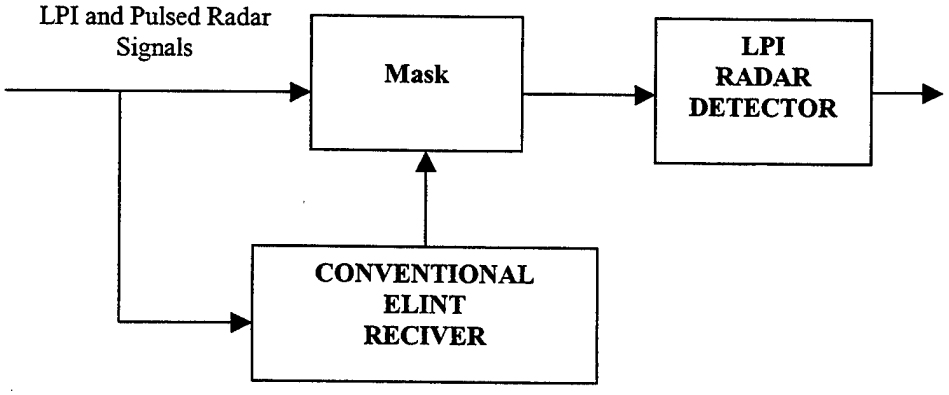

Figure 2.9 Masking of Conventional Pulsed Radar Signal

Through its normal function, the ELINT receiver first filtered out the conventional pulsed radar signals. The detected pulses are then masked. Due to the short period of conventional pulses (microseconds in comparison to LPI radar period of 1 millisecond), there will be minimal losses due to the masking effect [1]. However, the mask will not be included as part of the Digital LPI Radar Detector experiment's objective because of the unavailability of an actual ES receiver.

III. HARDWARE

A. HARDWARE SETUP

To verify the LPI radar detection capability, both the linear FMCW transmitter and the receiver with digital adaptive correlation detector were setup. The setup allows the actual reception of a linear-FMCW signal propagating through free space. Both transmitter and receiver hardware were built using commercially available components to facilitate future development, reduce setup cost, and for ease of eventual production.

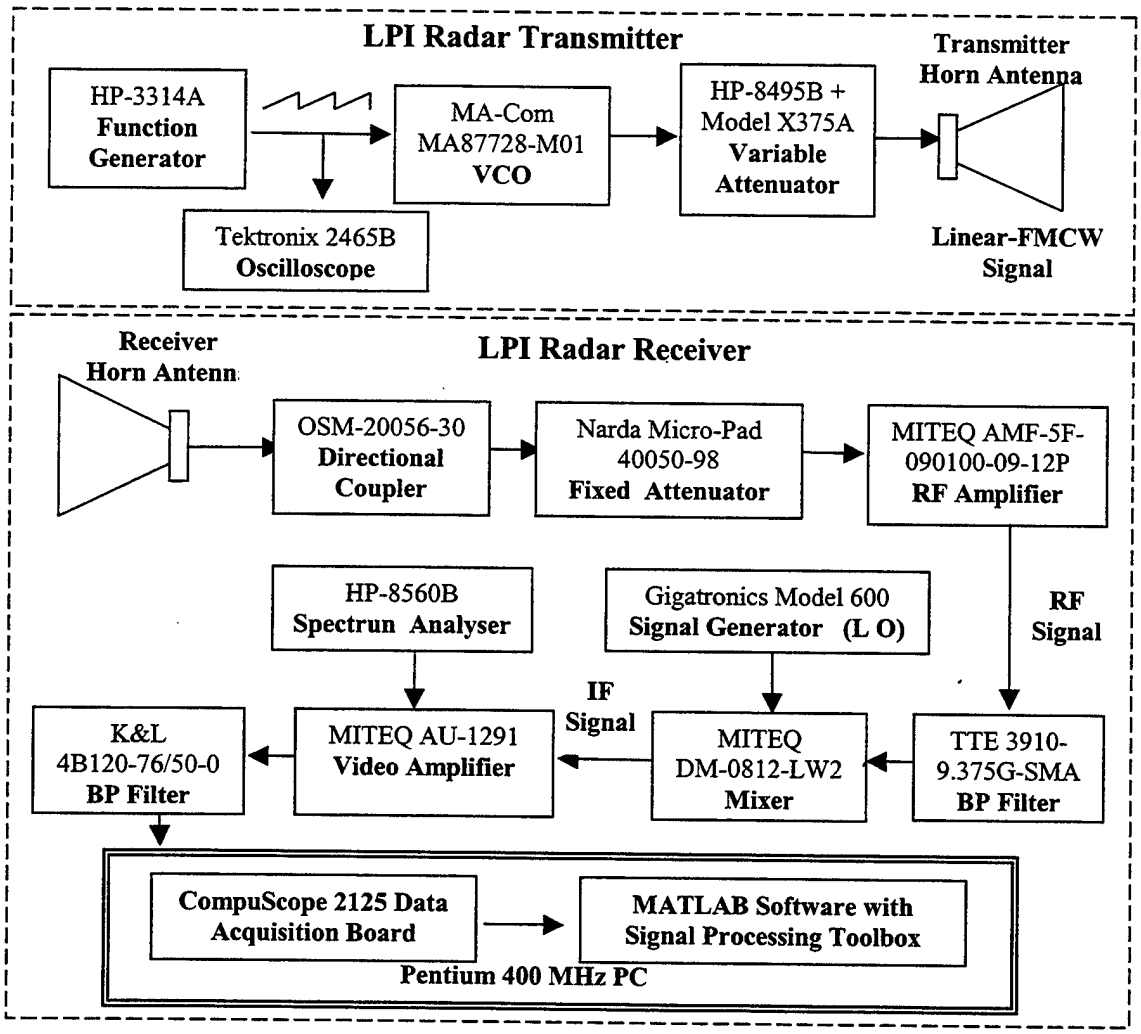

Figure 3.1 Hardware Setup Block Diagram

The hardware setups for testing the LPI radar detector are as shown in Figure 3.1 to Figure 3.3. Detailed specifications of the components, equipment and software are further elaborated in the subsections that follow.

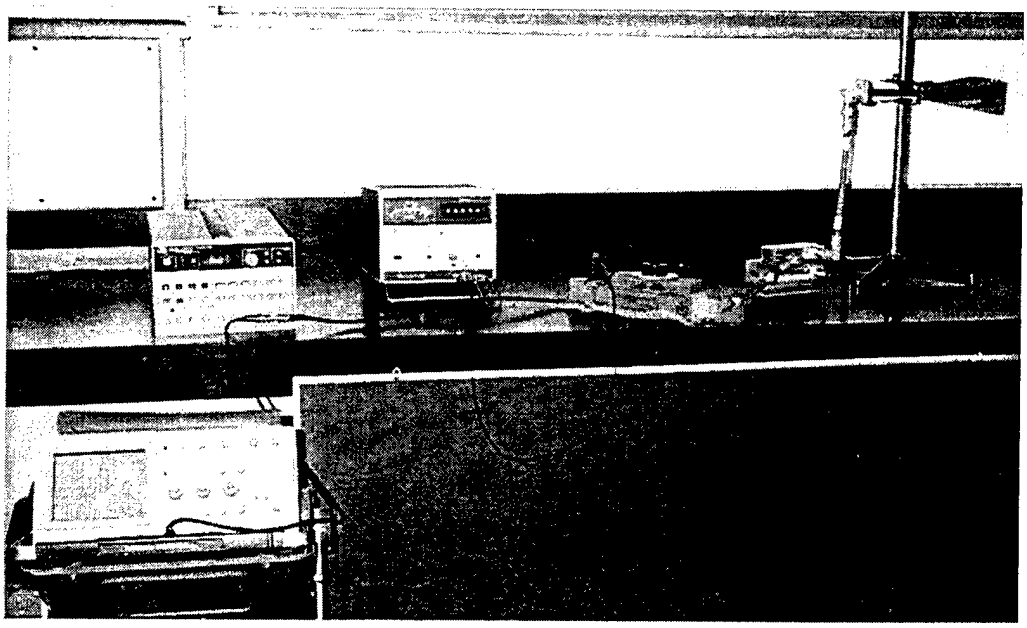

Figure 3.2 Transmitter Setup

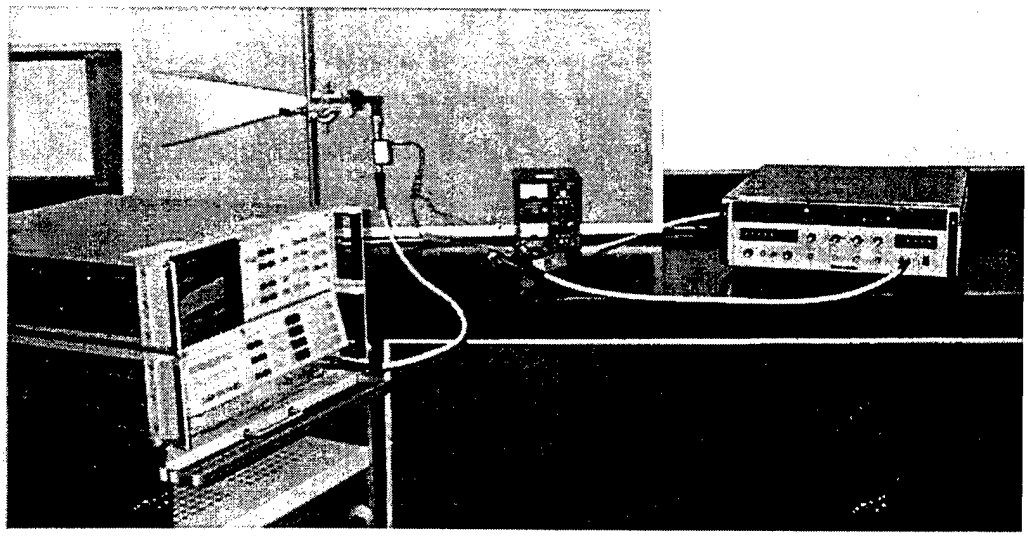

Figure 3.3 Receiver Setup

B. TRANSMITTER

1. Voltage Controlled Oscillator (VCO) Transceiver

A MA-COM MA87728-M01 varactor tuned X-band Gunn osicllator/transceiver was used to generate the linear-FMCW (chirp) signal at the transmitter. This low cost transceiver has a varactor tuned Gunn VCO that is capable of the required 50 MHz electronic frequency tuning. To achieve a millisecond linear-FMCW signal, a 1 kHz sawtooth waveform was applied to the electronic tuning bias input of the varactor. The Gunn VCO produces a low-power (10mW) linear-FMCW radar signal as described in Equation 2.1. The generated chirp signal was fed via a variable attenuator to a horn antenna which simulate the transmission of a LPI (Pilot/Scout) radar.

For the test, the various chirp bandwidths of the Pilot/Scout radar systems were generated. This was achieved by varying the amplitude of the 1 kHz sawtooth waveform input to the varactor. Using both mechanical frequency adjustment and electronic tuning bias of the transceiver, the center frequency of the chirp signal was tuned to 9.375 GHz, that of Pilot/Scout radar systems. Besides electronic tuning bias, a +8 Vdc fixed Gunn bias was also applied to the VCO for proper operations.

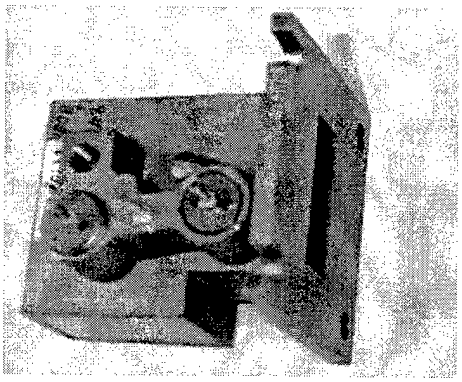

Figure 3.4 MA-COM MA87728-M01 Voltage Control Oscillator

2. Function Generator

A Hewlett-Packard Model-3314A function generator (Figure 3.5) was used to generate the 1 kHz sawtooth waveform needed by the Gunn VCO varactor for electronic tuning to generate the chirp signal. As this function generator is capable of up to only 95% sawtooth waveform symmetry offset (as shown in Figure 3.6; captured using a Tektronix 2465B oscilloscope), the transmitted chirp signal contains 0.95ms up-chirp and 0.05ms down-chirp. However, on the receiving end, the deramping signal at the LPI radar receiver contains negligible down-chirp (part of the digital deramping process). The effect of the down-chirp was subsequently found to be minimal.

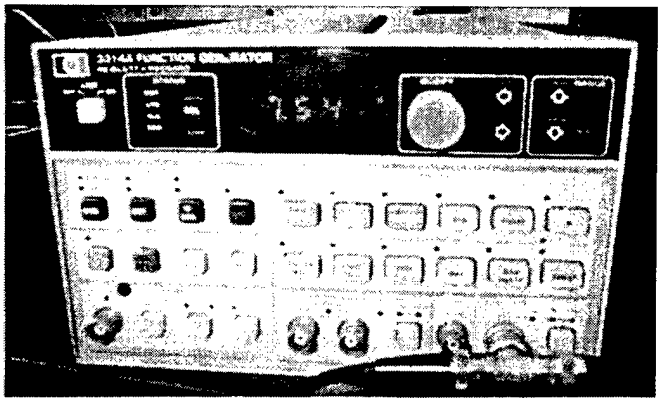

Figure 3.5 Hewlett-Packard Model-3314A Function Generator

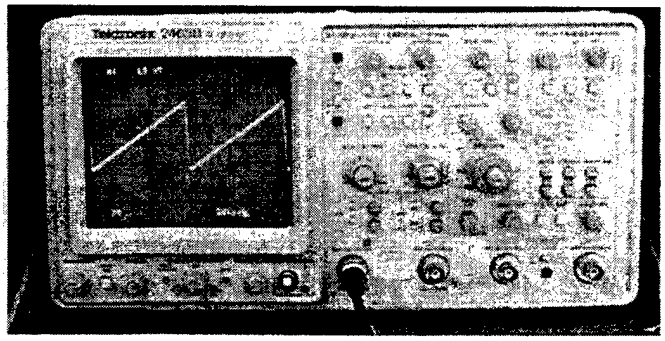

Figure 3.6 Tektronix 2465B oscilloscope

3. Variable Attenuator

To simulate varying signal power at the receiver due to different ranges of detection, the transmitted power was varied using variable attenuators. A combination of 2 variable attenuators, the HP model X375A (Figure 3.7) and HP8495B (Figure 3.8), was used to simulate the attenuation due to signal propagation through free space. The HP8495B variable attenuator can be adjusted from 0 to 70dB in steps of 10dB, while the X375A is adjustable continuously up to 20dB attenuation. Together, they can introduce continuous attenuation adjustment from 0 to 90dB. Accounting for the low power output of the VCO and the free-space loss, the received signal power in the laboratory setup was –30dBm. The signal power at the receiver can thus be varied continuously from –30dBm to –120dBm.

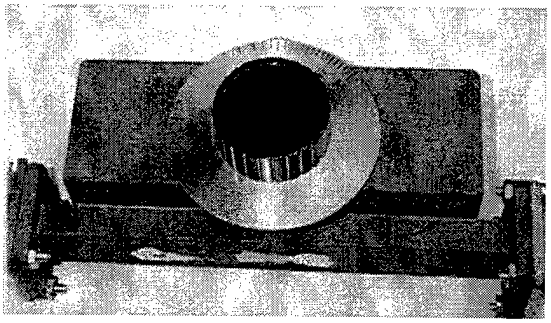

Figure 3.7 HP X375A Variable Attenuator

Figure 3.8 HP8495B variable attenuator

4. Antennas

Two standard horn antennas (Figures 3.9 and 3.10) were used in the experiment, one as the transmitter while the other the receiver. Since the parameter of interest is the signal power at the front end of the receiver, the gains of the antennas can be arbitrarily chosen. The performances of the antennas are therefore not a factor in the experiment.

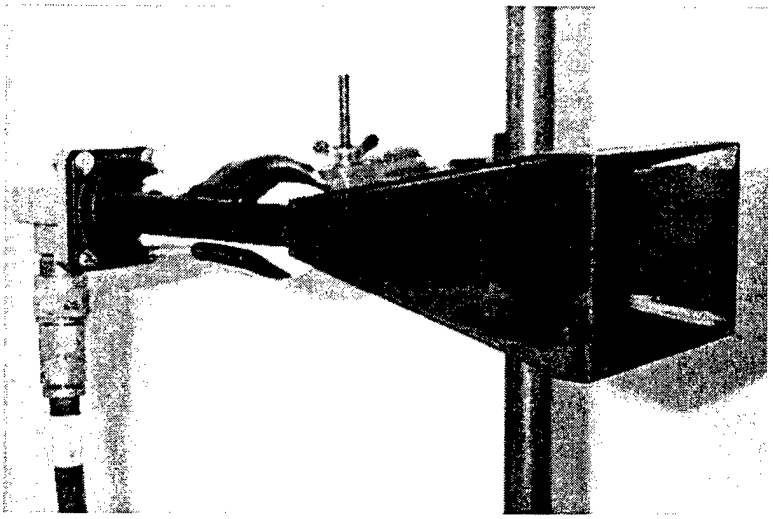

Figure 3.9 Transmitter Standard Gain Horn

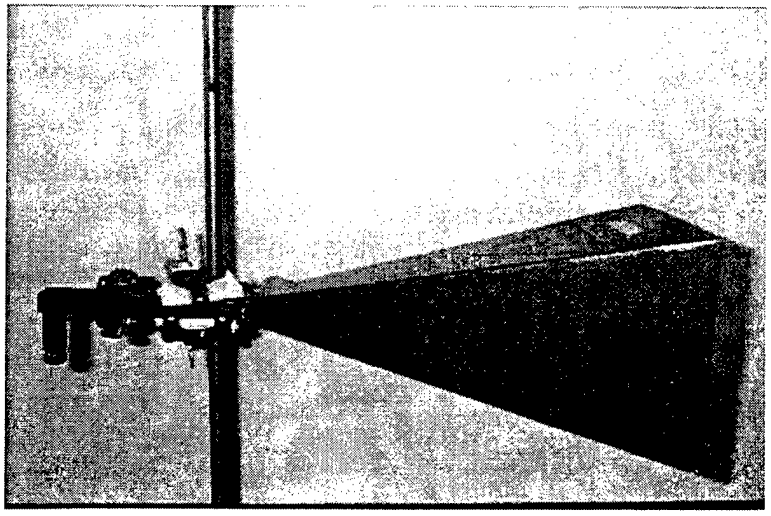

Figure 3.10 Receiver Standard Gain Horn

C. RECEIVER

1. Directional Coupler

The low-energy chirp signal at the front-end of the LPI radar detector has to be monitored to determine its power, center frequency and bandwidth. However, the power level of interest (–102dBm or less), is below the –65dBm resolution capability of the spectrum analyzer used. An Omni-Spectra model 50056-30 directional coupler, together with a Narda Micro-Pad 40050-98 fixed attenuator (Figure 3.11), was inserted at the front end to attenuate the received chirp signal before routing it to the input of the detector. They introduced a total attenuation of 49dB before the detector; 30dB and 19dB by the directional coupler and fixed attenuator respectively. The signal at the unattenuated end of the directional coupler is fed to a HP8566B Spectrum Analyzer (Figure 3.12). A –102 dBm signal at the input of the detector will then translate to a –53dBm power level at the spectrum analyzer. This setup thus allows the incoming chirp signal to be monitored using the spectrum analyzer while routing the required low-level signal of –102dBm to the detector.

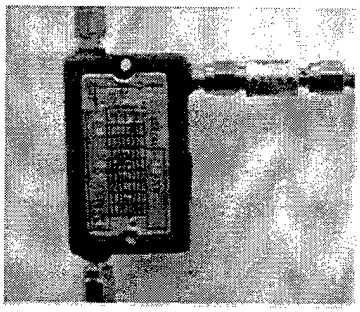

Figure 3.11 Omni-Spectra model 50056-30 Directional Coupler with Attenuator

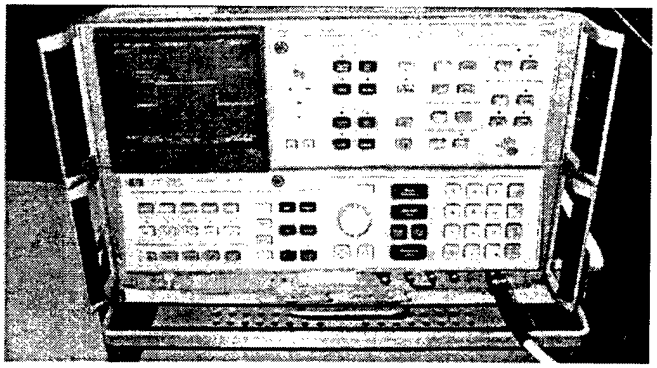

Figure 3.12 HP8566B Spectrum Analyzer

2. Low-Noise Amplifier

The received low-energy chirp signal, after routing through the directional coupler and fixed attenuator, was sent to the MITEQ Model-AMF-5F-090100-09-12P (Figure 3.13) low-noise amplifier (LNA) at the detector front-end. The LNA was placed in front of the detector to improve the overall system noise figure. It has a noise figure of 0.9dB and a gain of 39dB. The X-band LNA has an operating bandwidth of 1 GHz, from 9.0 GHz to 10.0 GHz. Its maximum passband response deviation is ±0.5 dB. For proper operation, it requires a power supply of +15 Vdc and draws a current of about 15 mA.

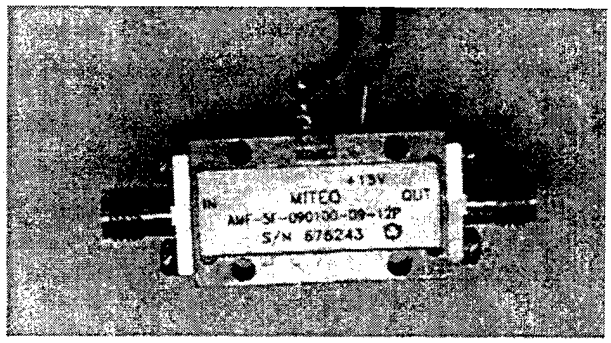

Figure 3.13 MITEQ Low Noise Amplifier

3. Bandpass Filter (RF Selection)

The TTE Model-K3910-9.375G-SMA bandpass filter (BPF) (Figure 3.14) was used a RF channel selector. It has a bandwidth of 300 MHz (9.225 GHz to 9.525 GHz) with a center frequency of 9.375 GHz. This BPF was chosen to simulate the tuning of the LPI receiver to the carrier frequency of the Pilot/Scout radar systems. The BPF introduces an insertion loss of 0.63dB (typical value). The 300MHz bandwidth selected is more than sufficient to pass the incoming chirp signal bandwidth of 50 MHz. The wider than required bandwidth was used in the experimental to cater for flexibility in laboratory testing. It allows for minor deviation in the center frequency without re-tuning. On the other hand, it passes a 300 MHz band of noise to the mixer. For a practical system, an optimal choice is to limit the passband to slightly larger than the maximum incoming signal bandwidth.

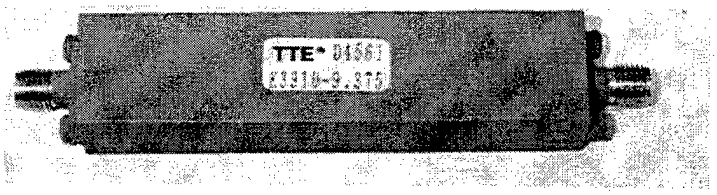

Figure 3.14 TTE Model-K3910-9.375G-SMA Bandpass Filter

4. Mixer and Local Oscillator

The mixer serves to translate the incoming RF signal (9.375 GHz) into an IF signal (75 MHz) suitable for the analog-to-digital converter (ADC). Stepping down to IF is essential to allow the use of a lower sampling rate of the ADC to prevent distortion due to aliasing. At lower sampling rate, the amount of captured data is reduced and processing time shortened. Mixing the signal down to base-band is not advisable as it will introduce distortion near the zero frequency (dc) region.

The LNA amplifies the incoming signal and boost it up to the level required by the mixer. Depending on the strength of the input signal, the signal strength at the mixer is about –56dBm (equivalent to –102dBm at front-end). In this experiment, MITEQ DM-0812-LW2 mixer was used (Figure 3.15). It introduced a loss of about 4.5dB. For the mixing process, a local oscillator (LO) signal power between 7 dBm and 13 dBm is required. A Gigatronics Model-600 microwave signal generator (Figure 3.16) was used as a LO. The LO power was set to +10dBm for all experiments conducted. Its frequency was tuned to 9.299 GHz to generate an IF signal centered at 76 MHz. For the largest bandwidth chirp signal of 50 MHz, the frequency band will be 51 MHz to 101 MHz. Hence, no DC signal was involved.

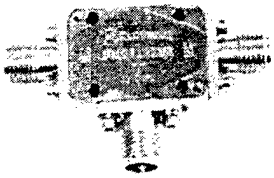

Figure 3.15 MITEQ DM-0812-LW2 Mixer

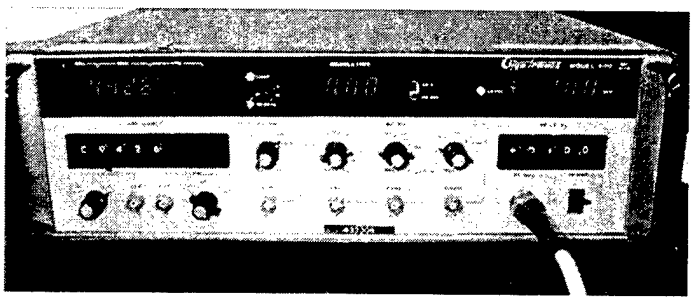

Figure 3.16 Gigatronics Model-600 Microwave Signal Generator

5. Video Amplifier

A MITEQ Model-AU-1291 video amplifier (Figure 3.17) was used to amplify the IF signal to the operating levels of the ADC. This amplifier has a gain of 62.7dB with a relatively flat passband (±0.5dB) of 500 MHz (from 0.01 to 500 MHz). It needs a DC power supply of +15 V and draws a current of about 89 mA .

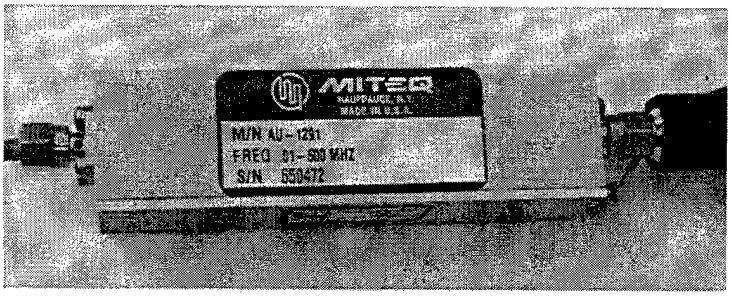

Figure 3.17 MITEQ Model-AU-1291 Video Amplifier

6. Bandpass Filter (IF Selection)

Before sampling, it is critical to limit the highest frequency and the bandwidth of the signal at the input of the ADC. This is essential to minimize distortion due to aliaing and to reduce the noise passing through the system. To achieve this, a K&L microwave Inc. 4B120-76/50-0 bandpass filter (Figure 3.18) was introduced after the video amplifier. It is a 4-pole tubular BPF with a center frequency of 76 MHz with a bandwidth of 50 MHz (51 MHz to 101 MHz). It introduces an insertion loss of 0.28 dB (typical). Aliasing is avoided since the BPF limits the highest frequency to below 125 MHz (half of the ADC sampling frequency of 250 MHz). At the same time, band-limiting the signal reduces the amount of noise passing through the system. This will in turn improve the overall signal-to-noise ratio.

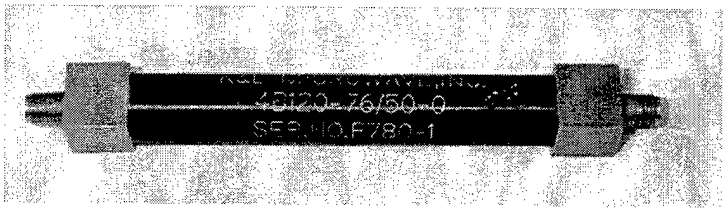

Figure 3.18 4B120-76/50-0 Bandpass Filter

D. OTHER HARDWARE REQUIRED

1. Power Supplies

The Gunn VCO requires a bias voltage of 8 Vdc while the LNA and the video amplifiers each require a 15 Vdc power supply. These are not depicted in the Figure 3.1. A HP6114A precision power supply catered to the +8 Vdc the Gunn VCO needed (Figure 3.19). Two HP Model-6216A power supplies were utilized to power the amplifiers (Figure 3.20).

Figure 3.19 HP6114A Precision Power Supply

Figure 3.20 HP Model-6216A Power Supply

2. Cables and Connectors

Low-loss, shielded microwave cables were used for components inter-connection to minimize losses and electro-magnetic interference (EMI). Cables of lengths ranging from 0.1 m to 1 m were used. These cables were terminated with SMA or Type-N connectors. Although the losses introduced by these cables and connectors are relatively small, they were included in the overall gain computation.

E. OVERALL SYSTEM GAIN CONSIDERATIONS

. The signal level at the input of ADC is critical to ensure that the smallest signal expected does not fall below the resolution capability of the ADC. Furthermore, to avoid distortion, the highest signal level should not exceed saturation limit of the ADC. To be certain, the overall system gain has to be determined. Based on the above setup, the overall system gain can be computed as follows:

$$G_{total} = G_{FE} + G_{LNA} + G_{BPF(r)} + G_{mixer} + G_{video\ amp} + G_{BPF(i)} + Loss\,(dB) \qquad (3.1)$$

$$G_{total} = (-1.01) + 46.0 + (-0.63) + (-4.5) + 62.7\,(-0.28) + (-2.8) = 99.48\ dB \qquad (3.2)$$

The overall noise figure of the system is computed for the system block diagram as shown in Figure 3.21:

$$F = F_1 + \frac{F_2 - 1}{G_1} + \frac{F_3 - 1}{G_1 G_2} + \frac{F_4 - 1}{G_1 G_2 G_3} + \frac{F_5 - 1}{G_1 G_2 G_3 G_4} \qquad (3.3)$$

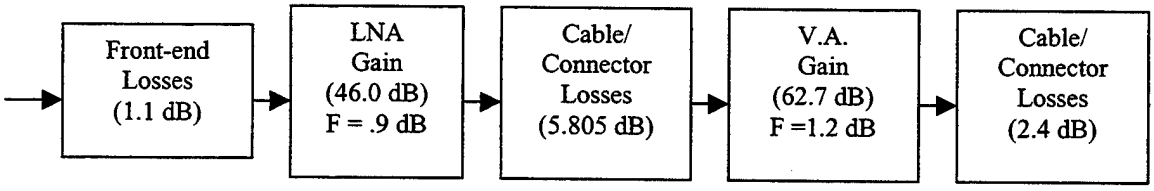

Figure 3.21 Noise Figure Block Diagram

$$
\begin{aligned}
F &= 1.29 + \frac{1.23-1}{0.775} + \frac{3.81-1}{0.775\times 39810} + \frac{1.32-1}{0.775\times 39810\times 0.262} \\
&\quad + \frac{1.74-1}{0.775\times 39810\times 0.262\times 1.86\times 10^{6}} \\
&= 1.59 \\
&= 2\,dB
\end{aligned}
\tag{3.4}
$$

Total system noise is computed to be –95 dBm.

$$
\begin{aligned}
N &= KTBF \\
&= 1.38\times 10^{-23}\times 290\times 50\times 10^{6}\times 1.58 \\
&= 3.16\times 10^{-13} \\
&= -95\,dBm
\end{aligned}
\tag{3.5}
$$

The threshold for detection at the output is based on a CFAR scheme that sets the signal-to-noise ratio at 2.56 dB. The minimum input signal strength that ensures detection (for the perfect deramping situation) is $S_{i(min)}$

$$
\begin{aligned}
F &= \frac{SNR_i}{SNR_o} \\
SNR_i &= F + SNR_o\ (dB) \\
&= 2 + 2.56\ dB \\
&= 4.56\ dB
\end{aligned}
\tag{3.6}
$$

$$
\begin{aligned}
S_i &= N + SNR_i \\
&= -90.44\ dB \\
S_{i(\min)} &= S_i - PG \\
&= -90.44 - 47\ dB \\
&= -137.44\ dB
\end{aligned}
\tag{3.7}
$$

A signal strength of –137.4 dBm corresponds to a –37.96 dBm signal at the input of the ADC. This is within the resolution capability of the ADC of –52.14 dBm; an equivalent level of –151.14 dBm at the front end of the detector. The maximum signal strength at the ADC before saturation occurs is 24 dBm. This translates to an input signal

strength of –75.0 dBm. Hence, the dynamic range of the system is –75.0 to –137.4 dBm. This is well within the expected range of input signal strength for the proposed experiment.

THIS PAGE INTENTIONALLY LEFT BLANK

IV. SOFTWARE

A. COMPUSCOPE 2125

The A/D conversion and data formatting of received signals are carried out by the Gage's CompuScope 2125 Data Acquisition Card installed onboard a Penium II 400 MHz desktop computer. Windows NT (release 4.0) is the Operating System used.

The CompuScope 2125 converts the analog voltage signals to digital signals at 8-bit resolution. The sampling rate is set at 250 Msps (or MHz) at a selectable voltage range 0.1 to 5 Volts.

The CompuScope 2125 card is controlled by MATLAB codes using Gage's CompuScope Software Development Kit (SDK). It allows MATLAB to communicate with the card's software drivers in order to specify the settings for the data acquisition.

The various parameter settings for the board are organized in the form of structures in the SDK. The parameters for the acquisition of data for this experiment are specified in the MATLAB code *setupcslpi.m*.

1. Sampling Rate

The CompuScope 2125 is capable of operating in dual-channel mode at sampling rates up to 125 Msps or in single-channel mode up at 250 Msps. With the maximum chirp bandwidth of the LPI at 50 MHz, using an Intermediate Frequency of 76 MHz, for reasons explained in Chapter II (and shown in Figures 2.7 and 2.8), the maximum frequency of interest is 101 MHz. As such, the sampling rate of 250 MHz is selected to prevent aliasing up to 125 MHz. The dual-channel mode will not satisfy the Nyquist Criteria.

2. Dynamic Range

The voltage range, V_r, for the card is selectable depending on the maximum power and resolution required. With the impedance set at 50 Ω, the maximum power before saturation at the input of the card is computed as follows:

$$P_{\max} = \frac{\left(V_r / \sqrt{2}\right)^2}{50\Omega} \tag{4.1}$$

Since the CompuScope card is an 8-bit A/D convertor, there are 128 quantization levels with one sign bit. The instantaneous dynamic range is 20 log(128) or 42.1 dB and the resolution is computed as follows:

$$P_{resolution} = \frac{\left(\frac{V_r}{128} / \sqrt{2}\right)^2}{50\Omega} \tag{4.2}$$

Quantization noise is computed based on half the voltage step. It is thus 6 dB below resolution. The voltage range chosen is the minimum without saturation so that the maximum amount of detail is captured.

The available V_r settings and their corresponding maximum power and resolution computed based on Equations 4.1 and 4.2 are tabulated in Table 4.1.

Voltage Range	Resolution in dBm	Maximum Power at LNA	Quantization Noise in dBm
0.10	-151.14	-109.00	-157.14
0.20	-145.12	-102.98	-151.12
0.50	-137.16	-95.02	-143.16
1.00	-131.14	-89.00	-137.14
2.00	-125.12	-82.98	-131.12
5.00	-117.16	-75.02	-123.16

Table 4.1 Maximum Power and Resolution of CompuScope 2125

B. MATLAB CODE

The MATLAB code *lpi_rcv.m* (enclosed in Appendix A) is written to carry out the digital deramping process. The received signal that is converted to digital signals is deramped using this code to determine if a FMCW radar, like the SCOUT or PILOT, is present. The program flow chart is shown in Figure 4.1.

1. Signal Capturing

Upon executing the code, the *capture_data.m* program (enclosed in Appendix B) is called to digitize the analog voltage signal received in Channel A of the CompuScope 2125 Data Acquisition Card settings specified in *setupcslpi.m.* (enclosed in Appendix C) The captured signal is saved as variable *sn*.

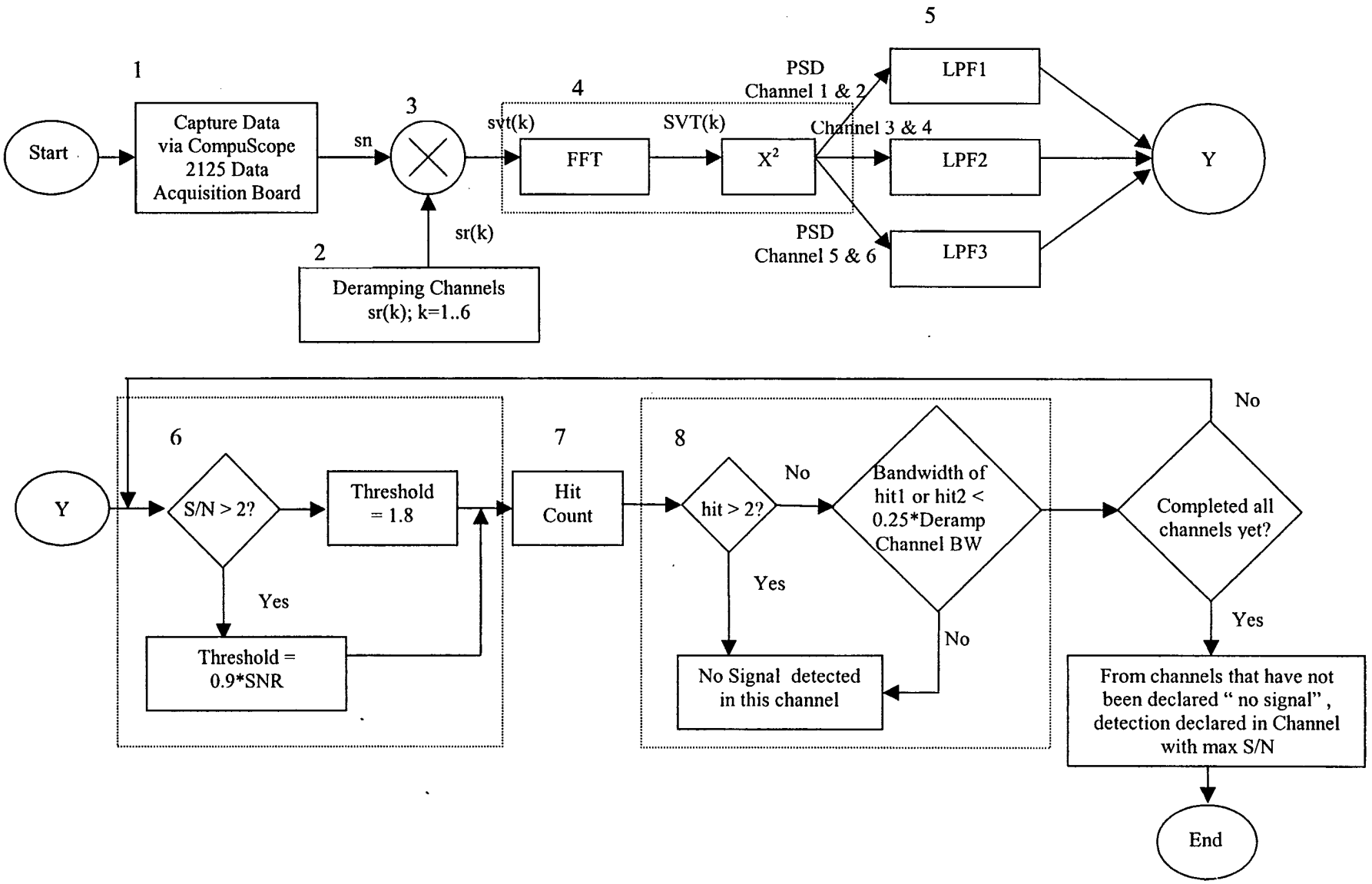

Figure 4.1 MATLAB Program Flow Chart

2. Deramping Channels

Six deramping channels are generated. The chirp bandwidth of each deramping channel is set in the code and can be changed relatively easily depending on the chirp characteristics or possible modes of the emitter of interest. In this case, the chirp bandwidth are set to match that of the PILOT radar's 6 modes of operation, namely 1.5625 MHz, 3.125 MHz, 6.25 MHz, 12.5 MHz, 25 MHz and 50 MHz respectively. The 6 deramping channels, *sr(k)*, are generated using complex exponentials to synthesize the In-phase (I) and Quadrature (Q) channels for optimum detection. The Power Spectral Density (PSD) of the deramping channels are shown in Figure 4.2.

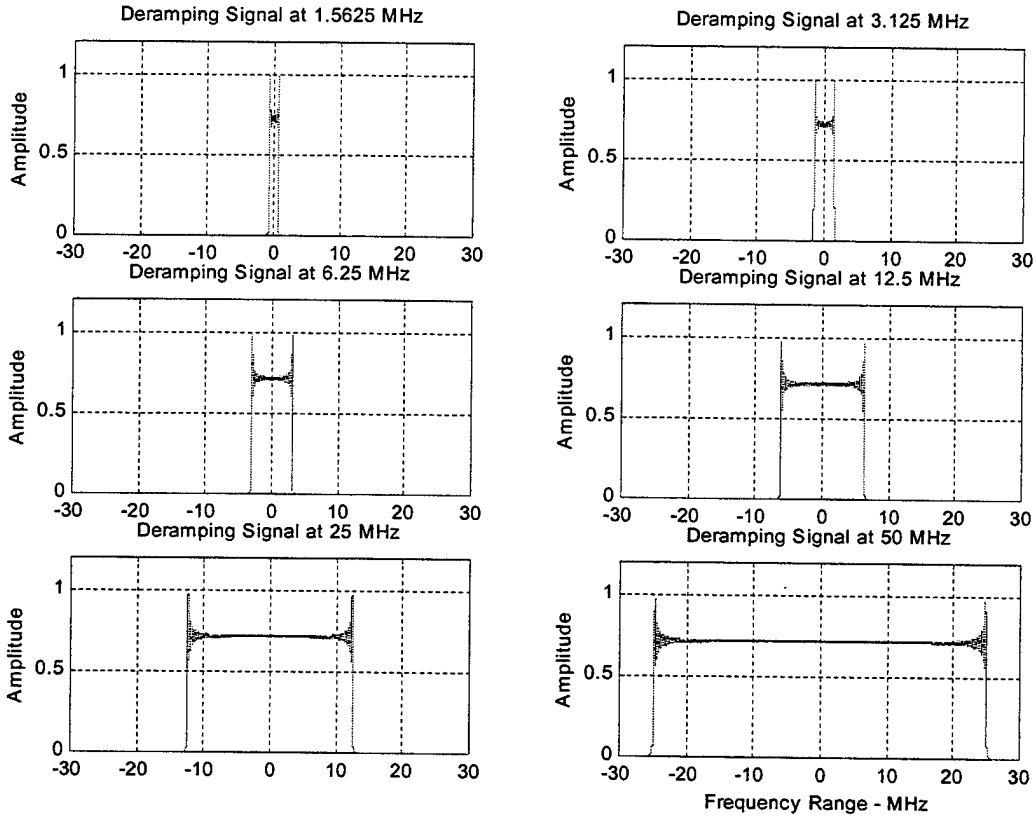

Figure 4.2 Chirp Bandwidth of Deramping Channels

3. Digital Deramping

The captured signal that is digitized by the A/D card is then deramped with each of the above 6 deramping channels to produce 6 resultant signals, *svt(k)*. The deramping process is carried out in MATLAB by multiplying the captured signal with the conjugate

values of the deramping signal in the time domain. Since complex exponentials are used, both the I and Q channels of the signal are deramped.

4. Power Spectral Density

A FFT is carried out on the deramped signal, *svt(k),* to obtain the voltages in the frequency domain. The normalized PSD is obtained by multiplying the respective channels by its own conjugate and dividing by the number of FFT points (in this case is 250000 points). The MATLAB command "fftshift" is also used to interchange the first and second quadrants with the third and fourth quadrants so that the spectrum can be centered on zero frequency. With a 50 MHz chirp input, the resultant PSD at the output of the 50 MHz deramp channel is shown in Figure 4.3.

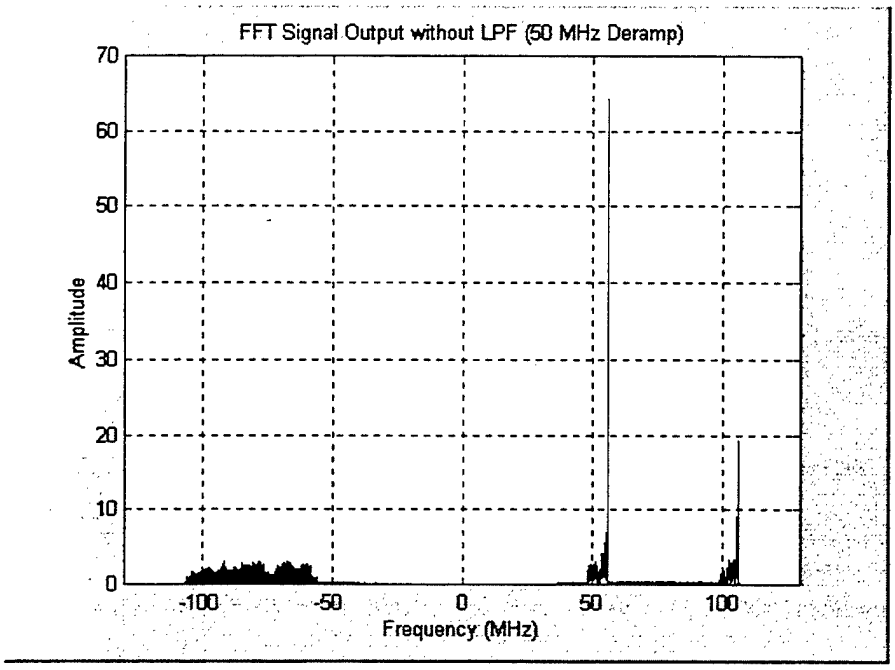

Figure 4.3 PSD of Deramped Signal (before LPF)

5. Digital Low Pass Filter

The PSD output of each channel is passed through a LPF to achieve the incoherent integration gain by suppressing the high frequencies noise. Since the resolution required for the 6 channels are different, the passband of the LPF is optimized for each channel. The PSD of Channels 1 and 2, Channels 3 and 4, and Channels 5 and 6

are passed through these filters LPF1, LPF2 and LPF3 respectively. Frequency response of the filters are shown in Figure 4.4. An example of an filtered PSD output (of Figure 4.3) is shown in Figure 4.5.

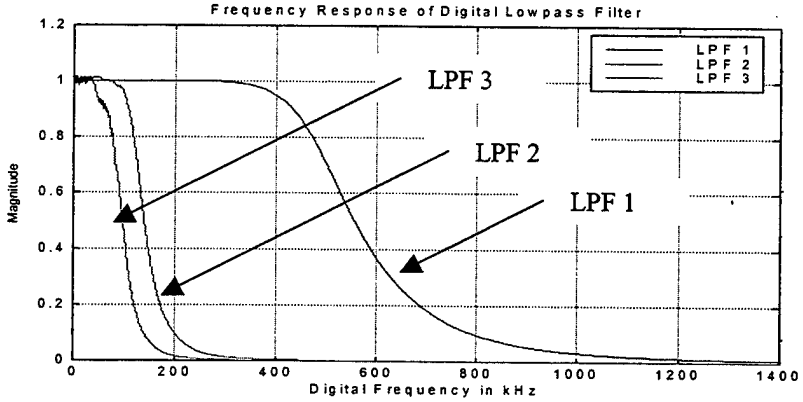

Figure 4.4 Frequency Response of Digital Lowpass Filters

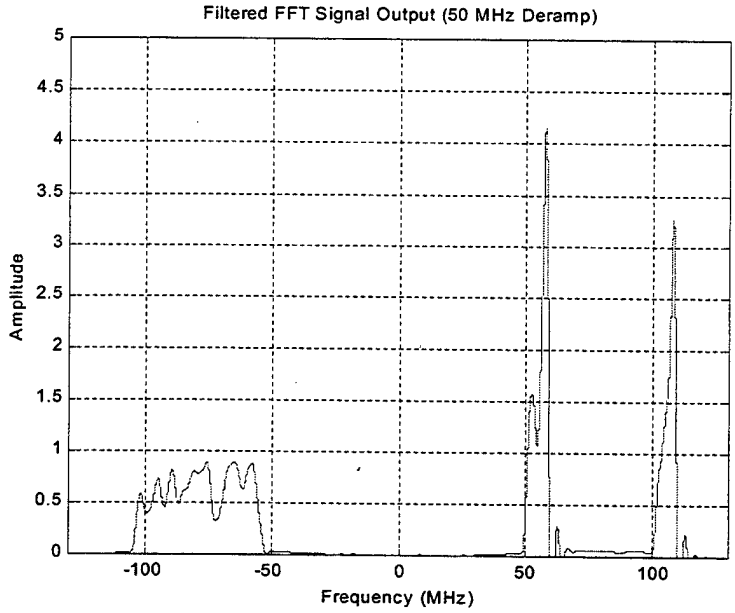

Figure 4.5 PSD of Deramped output after LPF

The incoherent integration gain is realized only when there is a slight mismatch between the FMCW Radar bandwidth and the preset channel bandwidth; especially when the SNR is very low since the energy is spread across a wider frequency band. Under such conditions, the LPF at selected cut-off frequencies effectively suppresses higher frequency noise thus enabling the channel with the closest match to have the highest

SNR. While the LPF reduces high frequency noise to enhance the performance of the detector in a mismatched situation, it reduces the overall SNR for a matched condition. This reduction however does not degrade the performance of the detector in a matched condition as there is always sufficient gain to separate the matched channel from the other channels.

6. Thresholding

Thresholding is carried out for each channel based on the a CFAR scheme where the threshold is set according to the local noise. The signal-to-noise level for each of the channels is computed by dividing the respective peak power with the average power in the channel.

$$SNR = \frac{P_{peak}(k)}{P_{average}(k)} \tag{4.3}$$

If the SNR is greater than 2, then

$$\text{Threshold(k)} = 0.9 * \text{SNR} * \text{mean(PSD(k))} \tag{4.4}$$

If the SNR is less than 2, then

$$\text{Threshold(k)} = 1.8*\text{mean(PSD(k))} \tag{4.5}$$

Adjacent frequency cells where the signal level crosses the threshold set are grouped together as a block, as can be seen in Figure 4.6.

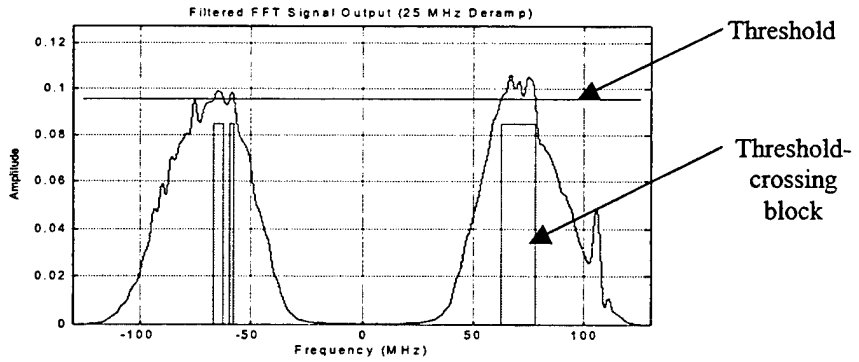

Figure 4.6 Example of Thresholding

7. Hit Counting

The number of blocks of continuous threshold crossing is counted for each channel. The following 2 conditions have to be met for a channel hit to be declared:

a. Threshold-crossing blocks are 2 or less

The number of threshold-crossing blocks resulting from a chirp signal is 2 or less. This condition is derived according to Equation 2.19. There should only be a maximum of 2 spikes in the event of any desynchronization in phase between the input signal and the matched filter. When only noise is present or when there is a severe mismatch in bandwidth, there will be multiple spikes resulting in many threshold-crossing blocks. Therefore, any channel with more than 2 threshold-crossing blocks is rejected as it is deemed that there is no chirp with bandwidth corresponding to this channel.

b. Block with less than 25% of channel's chirp bandwidth

For the channels that have 2 or less blocks, at least one block must be less than 25% of the respective deramping channel's bandwidth to be accepted. This occurs because, in a successful deramped output, there is at least one sharp peak.

In the cases when there is noise-only or when there is a pulse radar which slipped through the masking, the output can also result in 2 blocks of threshold-crossing signal. However, the widths of the threshold-crossing blocks are close to the respective deramping channel bandwidths. The phenonena can be seen in Figure 5.6 showing the deramped results of a pulse radar operating at 9.39 GHz and pulse width of 0.04 μs. Thus, this criteria helps to prevent noise-only channels from being passed as a chirp signal.

8. Channel Selection

A hit is declared in the channel with the highest SNR among the accepted channels. If none of the 6 channels passed the 2 tests, then it is declared that there is no chirp signal at all regardless of the signal-to-noise ratios of the deramped signals.

THIS PAGE INTENTIONALLY LEFT BLANK

V. RESULTS AND ANALYSIS

A. MODE DETERMINATION

1. Matched Signal

If the chirp bandwidths in the various modes of the FMCW LPI radar of interest are known, it can be set in all the deramping channels. Each channel will yield a result when deramped with the signal containing the radar of interest. The channel that has the same chirp bandwidth, as the mode of operation that the radar is operating in, will yield a distinct spike (or 2 if the phase is not synchronized) and will have the best signal-to-noise ratio. As shown in Figure 5.1, both channels 1 and 2 produced a single threshold-crossing spike. However, the channel with the correct bandwidth will yield the highest SNR. In this case, the FMCW LPI radar operating at 1.5625 MHz bandwidth produced a more distinct spike and has the best SNR in Channel 1 (charts are scaled to 1.2 times the corresponding channel's peak value).

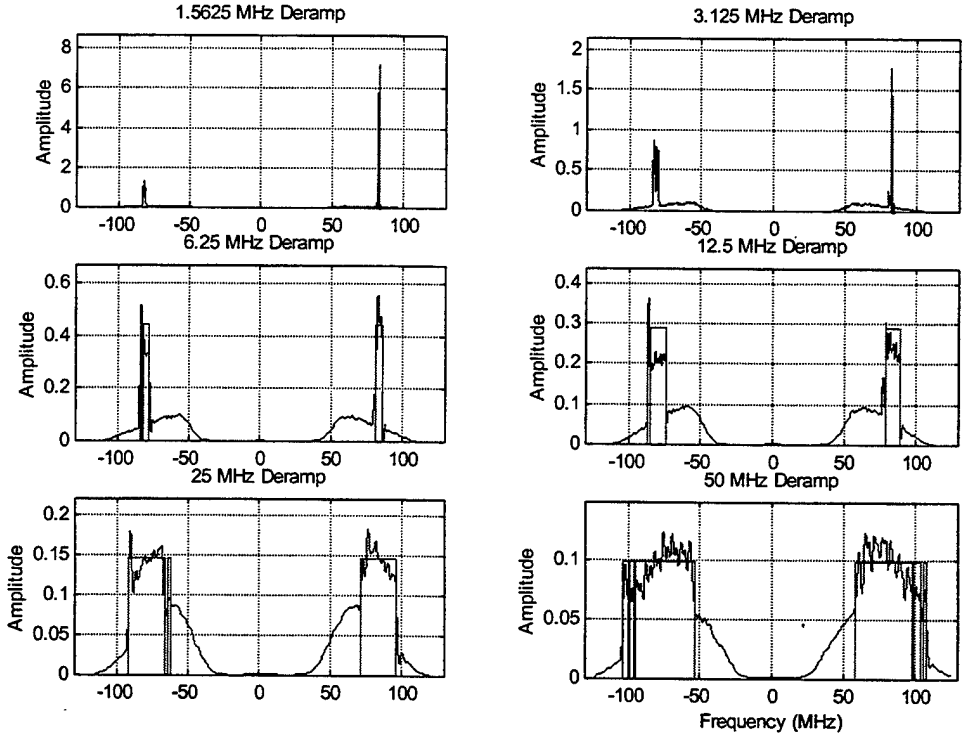

Figure 5.1 Deramped Output of a 1.5625 MHz Bandwidth FMCW Signal

Similarly, the LPI radar operating at 50 MHz produced the best deramped result in Channel 6 as in Figure 5.2. As discussed in Chapter II (Equation 2.17), Channel 6 which has the same chirp bandwidth completely deramps the LPI radar and thus produces a single-tone signal at the carrier frequency. In this case, the carrier frequency is the Intermediate Frequency. Other mode detection results can be found in Appendix D.

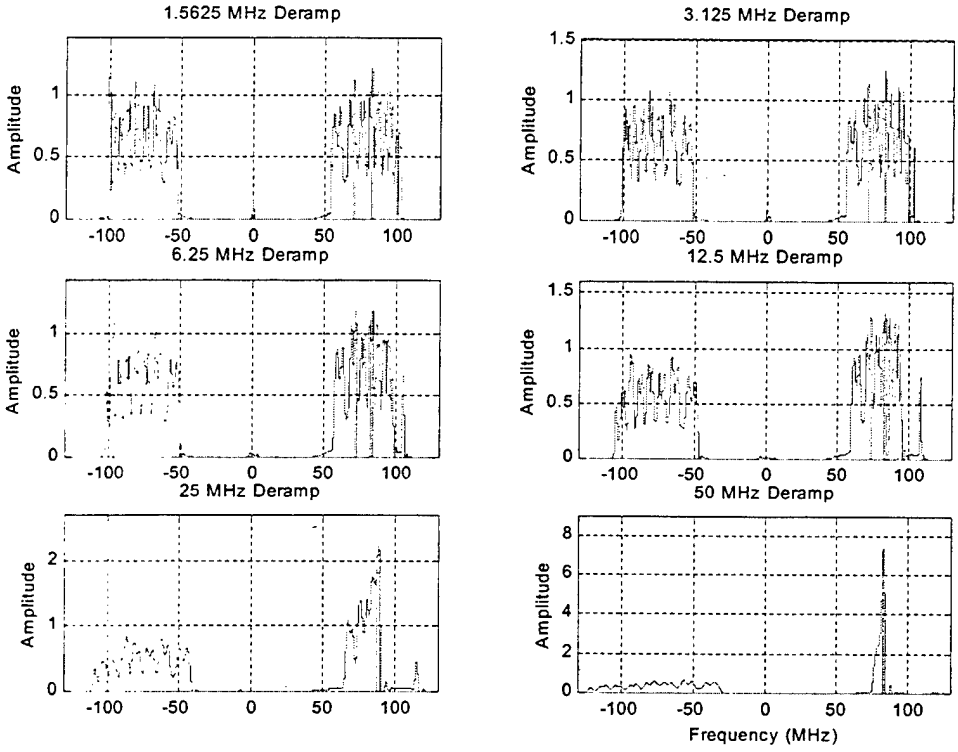

Figure 5.2 Deramped Output of a 50 MHz Bandwidth FMCW Signal

2. Chirp Bandwidth Mismatch

When there is a mismatch in the chirp bandwidth, the channel with a deramping bandwidth closest to the FMCW signal will produce the best signal-to-noise ratio. As can be seen in Figures 5.3 and 5.4, the 30 MHz FMCW produced a hit in the 25 MHz channel while the 40 MHz chirp produced a better result in the 50 MHz channel.

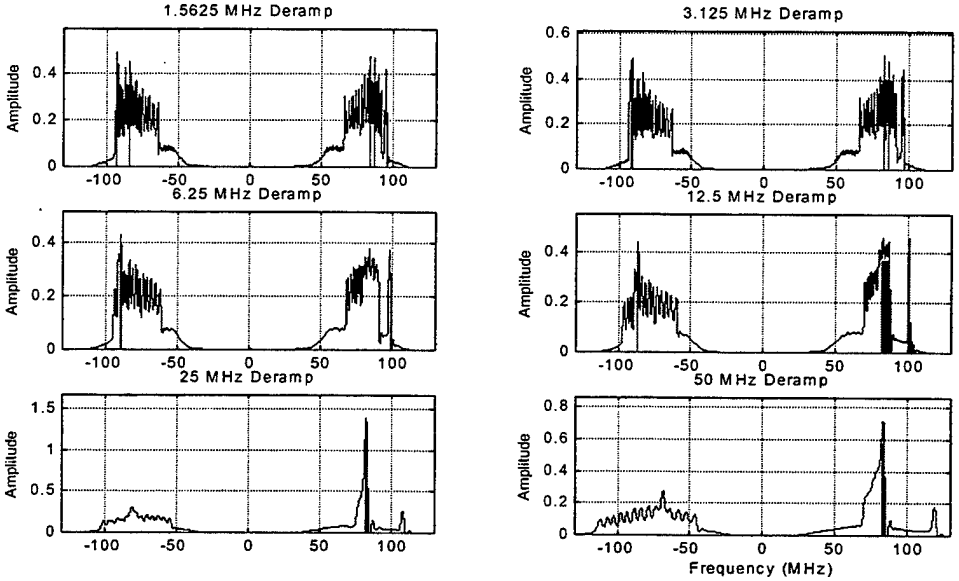

Figure 5.3 Deramped Output of a 30 MHz Bandwidth FMCW Signal

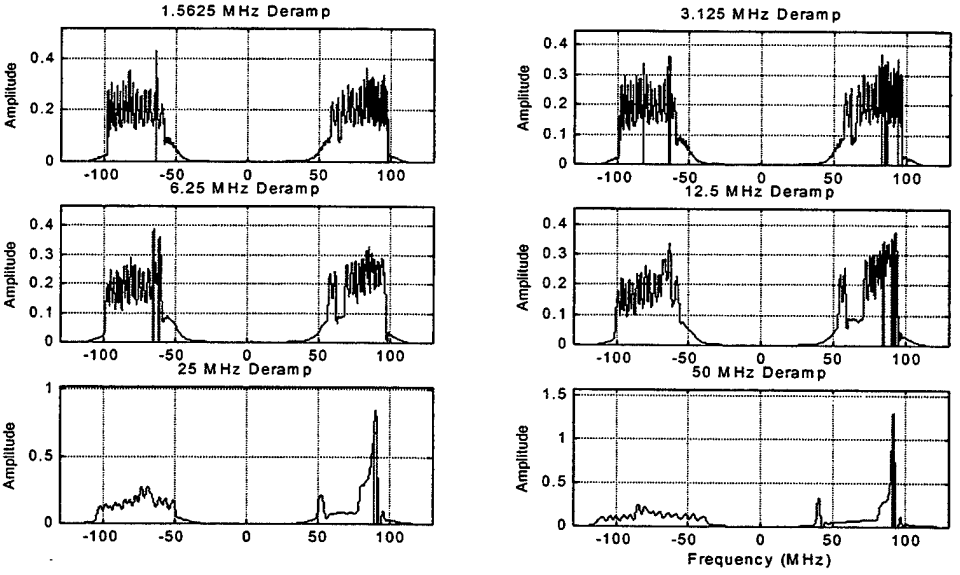

Figure 5.4 Deramped Ouput of a 40 MHz Bandwidth FMCW Signal

3. No Signal

When only noise is present, none of the channels produce any useful results and thus the system concludes that no signal is detected. In the event that the FMCW signal is too weak to be detected, it will yield the similar results.

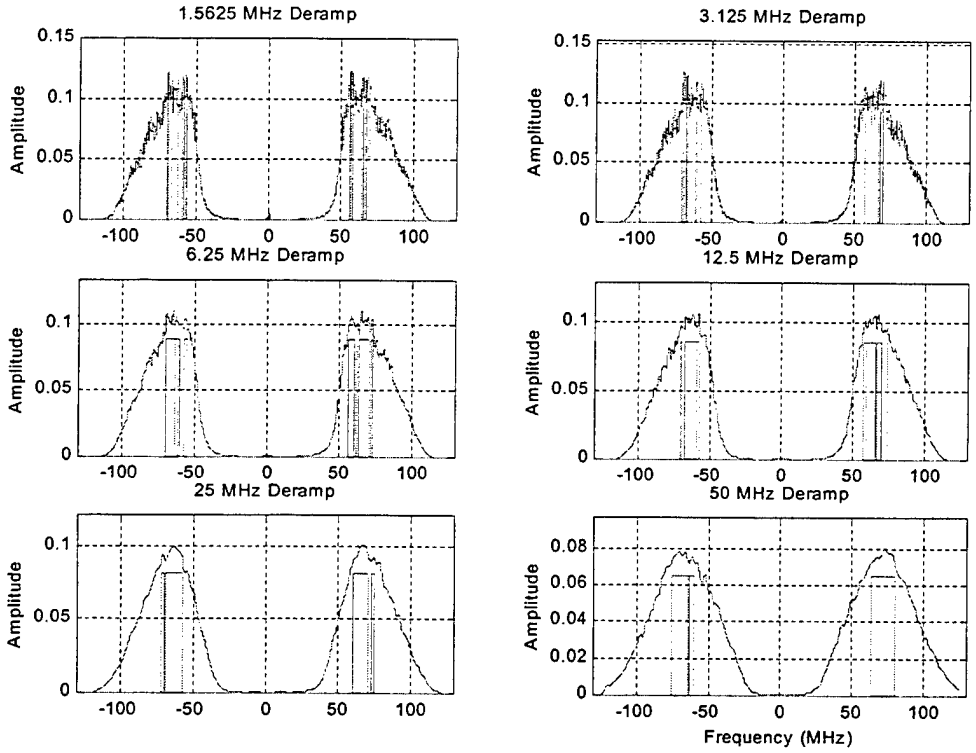

Figure 5.5 Deramped Output of Noise-Only Signal

4. Pulse Radar

In the presence of a pulse radar, the deramped results yielded two threshold-crossing blocks. This will meet the first condition for channel hit (Chapter 4, Section 7a). However, the widths of the blocks are close to the corresponding channel's deramping bandwidth, thus failing the second condition (Chapter 4, Section 7b). Therefore, these crossings are rejected and the conclusion is that no FMCW radar is present.

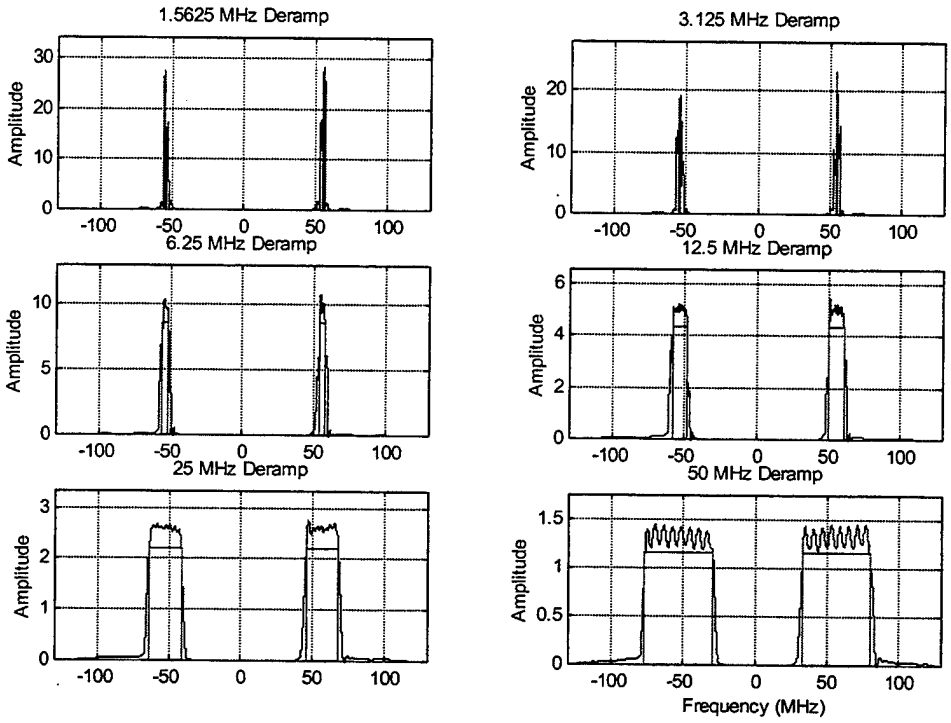

Figure 5.6 Deramped Output of a Pulse Radar

B. UNSYNCHRONIZED SIGNALS

As discussed in Chapter II and demonstrated in Equations 2.17, 2.18 and 2.19, when the incoming FMCW signal is synchronized with the internally generated chirp signal, the deramped result is a single-tone signal (Figure 5.7a) while an unsynchronized situation results in a two-tone deramped signal (Figure 5.7b). The greater the difference between the two peaks, the closer it is to being synchronized. The loss in signal SNR due to being unsynchronized in this case was 2.6 dB. It is determined that the maximum loss when totally unsynchronized is 3 dB since the energy is distributed between two peaks instead of one.

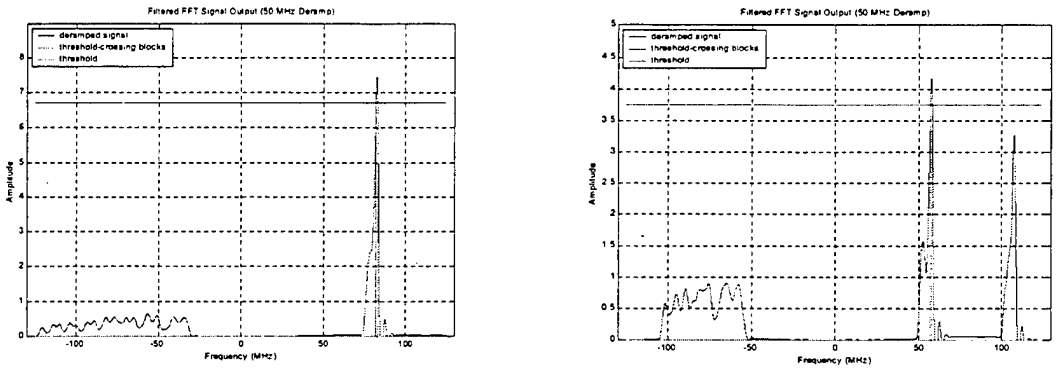

Figure 5.7 Deramped Output of 50MHz FMCW (a) Synchronized (b) Unsynchronized

The single-tone peak is located at the carrier frequency which is the Intermediate Frequency in our cases. However, as the LPI radar signal is time-shifted to be unsynchronized with the internally generated chirp, the deramped result transits into a two-tone signal and shifts slowly away from the carrier frequency. This process can be observed in Figure 5.8 and is described in Chapter II. When the LPI radar is completely de-synchronized with the internal chirp, the two peaks should be of equal magnitude, and centered on the carrier frequency. The two-tone signal always maintains a frequency separation that is equal to the chirp bandwidth of the LPI radar.

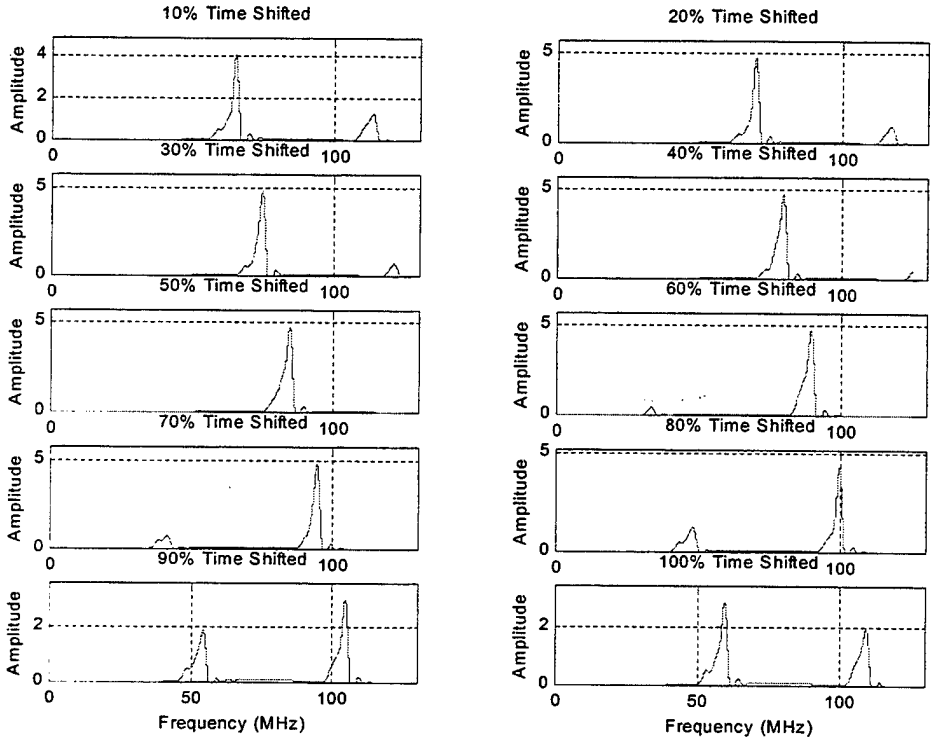

Figure 5.8 Deramped Output of 50MHz FMCW Shifted in Steps of 10% of Pulse Duration

C. DETECTION

1. Weak Signals

When the FMCW signal is very weak, the spike in the deramped output becomes less distinct and eventually disappears into the noise as the signal weakens. Figure 5.9a shows a deramped output in the 50 MHz channel of a FMCW signal at –103.8 dBm with a more prominent spike than that which is in Figure 5.9b where the signal is –108.2 dBm. The amplitude of the latter is also much lower.

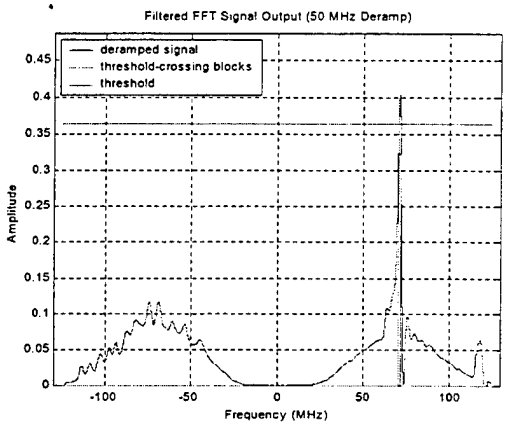

(a) –103.8 dBm

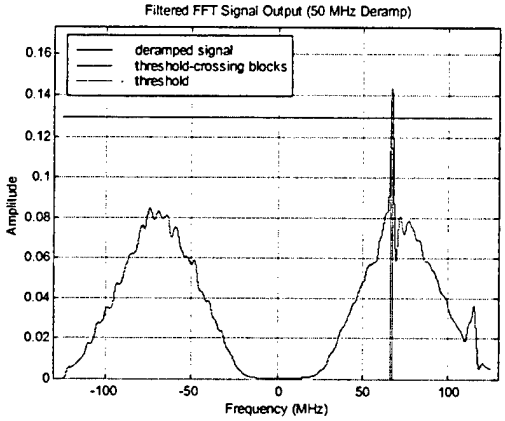

(b) –108.2 dBm

Figure 5.9 Deramped Output of Weak Signals

2. Detection Capability

The Digital LPI Receiver is tested for its capability to detect weak signals. The weakest FMCW signal successfully deramped for each of the modes of the PILOT radar is compiled in Table 5.1. Based on the four known transmitter power settings, the likely range of the transmitter is determined using the following:

$$R = \sqrt{\frac{P_t G_t G_r \lambda^2}{P_r L (4\pi)^2}} \tag{5.1}$$

R = Range of LPI Radar
Transmitter Power, P_t = 1 W, 100 mW, 10 mW, 1 mW
LPI Radar Antenna Sidelobe Gain, G_t = 16 dB
Detector Antenna Gain, G_r = 0 dBi
LPI Radar Wavelength, λ = 0.032 m
Polarization Loss, L = 3 dB

Bandwidth (MHz)	Received Power (dBm)	Detection Range (km) Corresponding to Tx Pwr (dBm)			
		1 W	100 mW	10 mW	1 mW
50	-108.20	92.46	29.24	9.25	2.92
25	-110.00	113.75	35.97	11.37	3.60
12.5	-112.60	153.44	48.52	15.34	4.85
6.25	-113.50	170.19	53.82	17.02	5.38
3.125	-115.20	206.99	65.45	20.70	6.55
1.5625	-123.00	508.09	160.67	50.81	16.07

Table 5.1 LPI Receiver Detection Ranges

From Table 5.1, it can be deduced that, when the LPI radar is transmitting at 1 W, the detection ranges of the Digital LPI Receiver is limited by the radar horizon as the detection ranges are beyond the horizon.

According to Equation 3.7, the sensitivity of the system setup is –137.44 dB with reference to the 50 MHz bandwidth chirp. With every reduction of half the bandwidth, there is a 3 dB reduction in sensitivity based on the time-bandwidth product. The theoretical sensitivity of each channel is tabulated with the practical sensitivity in Table 5.2.

Bandwidth (MHz)	Theoretical Sensitivity (dBm)	System Sensitivity (dBm)
50	-137.4	-108.20
25	-134.4	-110.00
12.5	-131.4	-112.60
6.25	-128.4	-113.50
3.125	-125.4	-115.20
1.5625	-122.4	-120.00

Table 5.2 Theoretical and Practical System Sensitivity

While we are able to achieve the theoretical sensitivity in the 1.5625 MHz chirp, the sensitivity of the system falls further and further behind the theoretical values as the chirp bandwidth increases.

We are not able to achieve the theoretical sensitivity because the transmitted linear ramp has a 95% up chirp and a 5% down chirp while the software synthesized chirp is effectively 100% up chirp and no down chirp. This mismatch in chirp waveform results in more losses in the larger bandwidth channels than that of the smaller ones. For example, the mismatch of 5% in the 50 MHz channel corresponds to a 2500 kHz bandwidth deramp output while that of a 1.5625 MHz channel is only 78 kHz. The deramp output energy is thus spread across a wider bandwidth for a 50 MHz channel than a 1.5625 MHz channel. As a result, the SNR for wider bandwidth channels suffer greater losses as compared to the lower bandwidth channels. In summary, it is more difficult to construct a matched filter for larger chirp bandwidth waveforms.

With the sensitivity obtained, it is shown that with the use of this digital deramping technique, the ES Receiver regains the range advantage over the LPI radar by defeating the design concept of the LPI radar.

VI. CONCLUSIONS AND RECOMMENDATIONS

A. CONCLUSIONS

The experimental results demonstrated the effectiveness of the Digital LPI Radar Detector in providing operationally significant detection ranges. Additionally, it is capable of determining the LPI radar's mode of operation and thus its range based on the signal strength received. The experiments also verified that it is more difficult to detect a chirp signal with a larger bandwidth than one with a smaller bandwidth. Nevertheless, based on a chirp signal with a 50 MHz bandwidth (the largest of the PILOT radar), the proposed Digital LPI Radar Detector achieved a range advantage over the transmitter even when the deramping filter was mismatched to the input signal waveform.

In comparison with an analog system, the Digital LPI Radar Detector offers flexibility in processing with the advantage of having only to capture the signal once. An adaptive matched filter could be achieved more readily using software re-tuning than analog adjustments which require the LPI radar signal to be present throughout the process.

B. RECOMMENDATIONS

With the successful laboratory testing of the Digital LPI Radar Detector, the proposed setup could be adapted to develop an operational piggyback detector for an existing ES receiver (such as the SLQ-32). As a furtherance of this project, the introduction of a temporal mask can be examined. Incorporation of a data base for know operational modes of LPI radars and frequency scanning to cover a broader band of carrier frequencies can also expand the capability of the system. The Digital LPI Radar Detector software algorithm can be refined to include automatic phase synchronization of the matched filter that will improve the SNR. This will in-turn facilitate the prospect of incorporating an algorithm to generate an adaptive matched filter for unknown operating modes (through the interpolation of the bandwidth between two channel matched filters).

THIS PAGE INTENTIONALLY LEFT BLANK

LIST OF REFERENCES

[1] D. C. Schleher, "Detection of LPI Radar Signals," Prepared for Center for Reconnaissance Research, Naval Postgraduate School, December 1999.

[2] D. C. Schleher, "Detection of LPI Radar Signals," 43rd Annual Joint Electronic Warfare Conference, Colorado Springs, April 28, 1998.

[3] Forecast International /DMS Market Intelligence Report, *Radar Forecast*, Scout and Pilot, July 1995.

[4] D. C. Schleher, "Low Probability of Intercept Radar," IEEE International Radar Conference, May 1985.

[5] August W. Rihaczek, *Principles of High Resolution Radar*, Artech House, Norwood, MA, 1996.

[6] Phillips Pilot-Covert Naval Radar, *International Defense Review*, September 1988.

[7] D. C. Schleher, *Electronic Warfare in the Information Age*, Artech House, Norwood, MA, 1999.

THIS PAGE INTENTIONALLY LEFT BLANK

APPENDICES

A. DERAMPING SOFTWARE (MATLAB CODE)

```
% Program Name : lpi_rcv.m
% MATLAB m-script file written for the software portion of
% the Digital LPI Detector
% the program does the following:
% 1. Captures the data using A/D card
% 2. Generates Chirps for Deramping Channels
% 3. Carry out deramping of captured signal with signals generated
% 4. Carry out FFT on outputs
% 5. Square the resultants
% 6. Put the results through a LPF
% 7. Plot the following:
%     a. Results after LPF
%     b. Threshold level
%     c. Threshold-crossing blocks
% 8. Outputs the selected SNR of each channel
% 9. Selects the Channel which has the best deramp result
%%%%%%%%%%%%%%%%%%%%%%%%%%%%%%%%%%%%%%%%%%%%%%%%%%%%%%%%%%%%%%%%%%%%%%%%

format compact;

%%%%%%%%%%%%%%%%%%%%%%%%%%%%%%%%%%%%%%%%%%%%%%%%%%%%%%%%%%%%%%%%%%%%%%%%
%%%                        A/D Convertion                                %%%
%%% ========================================================== %%%
%%%                  captures and transfers data                         %%%
%%%              from the CompuScope 2125 channel A                      %%%
%%%                        to vector sn                                  %%%
%%%%%%%%%%%%%%%%%%%%%%%%%%%%%%%%%%%%%%%%%%%%%%%%%%%%%%%%%%%%%%%%%%%%%%%%

capture_data;              %calls program to capture data of A/D converter
sn=sn(1:250000);           %ensures input signal length to be 120k points
sn=sn';                    %transpose sn to a column vector since FFT
                           %in Matlab is carried out on columns
T=1e-3;                    %Duration of each chirp pulse
lfft=250000;               %Input FFT Points
t=-T/2:T/(lfft-1):T/2;     %Set Time Base and Compute Parameters
t=t';                      %transposes t to a column vector

%%%%%%%%%%%%%%%%%%%%%%%%%%%%%%%%%%%%%%%%%%%%%%%%%%%%%%%%%%%%%%%%%%%%%%%%
%%%          Building the Deramping Channels                             %%%
%%%%%%%%%%%%%%%%%%%%%%%%%%%%%%%%%%%%%%%%%%%%%%%%%%%%%%%%%%%%%%%%%%%%%%%%
bws(1)=1.5625e6;      %Bandwidth of Deramp Channel 1
bws(2)=3.125e6;       %Bandwidth of Deramp Channel 2
bws(3)=6.25e6;        %Bandwidth of Deramp Channel 3
bws(4)=12.5e6;        %Bandwidth of Deramp Channel 4
bws(5)=25e6;          %Bandwidth of Deramp Channel 5
bws(6)=50e6;          %Bandwidth of Deramp Channel 6
n=length(bws);        %determine the number of channels
```

```
%%%%%%%%%%%%%%%%%%%%%%%%%%%%%%%%%%%%%%%%%%%%%%%%%%%%%%%%%%%%%%%%%%
%%%           Deramping carried out in the                     %%%
%%%        Time Domain by mixing the captured signal           %%%
%%%           with each deramping channel                      %%%
%%%%%%%%%%%%%%%%%%%%%%%%%%%%%%%%%%%%%%%%%%%%%%%%%%%%%%%%%%%%%%%%%%
for k=1:n,
   sr(:,k)=exp(j*pi*bws(k)*t.*t/T); %to generate deramping channels
   svt(:,k)=sn.*conj(sr(:,k));      %mixing/deramping
end

%%%%%%%%%%%%%%%%%%%%%%%%%%%%%%%%%%%%%%%%%%%%%%%%%%%%%%%%%%%%%%%%%%
%%%              Definition of constants                       %%%
%%%%%%%%%%%%%%%%%%%%%%%%%%%%%%%%%%%%%%%%%%%%%%%%%%%%%%%%%%%%%%%%%%
l=length(sn);
f=(1/T)*(-(l-1)/2:(l-1)/2);    %frequency span
fmax=130e6;                    %Scaling for x-axis

%%%%%%%%%%%%%%%%%%%%%%%%%%%%%%%%%%%%%%%%%%%%%%%%%%%%%%%%%%%%%%%%%%
%%%              FFT of Deramped output                        %%%
%%%%%%%%%%%%%%%%%%%%%%%%%%%%%%%%%%%%%%%%%%%%%%%%%%%%%%%%%%%%%%%%%%
ZY=fft(svt,lfft);
for k=1:n,
   Y(:,k)=fftshift(ZY(:,k));
end

%%%%%%%%%%%%%%%%%%%%%%%%%%%%%%%%%%%%%%%%%%%%%%%%%%%%%%%%%%%%%%%%%%
%%%                PSDs of Deramped Signal                     %%%
%%%         (Output of each deramping channels)                %%%
%%%%%%%%%%%%%%%%%%%%%%%%%%%%%%%%%%%%%%%%%%%%%%%%%%%%%%%%%%%%%%%%%%
Psd=Y.*conj(Y)/lfft;
A=ceil(max(Psd));

%%%%%%%%%%%%%%%%%%%%%%%%%%%%%%%%%%%%%%%%%%%%%%%%%%%%%%%%%%%%%%%%%%
%%%                    Low Pass Filter                         %%%
%%%%%%%%%%%%%%%%%%%%%%%%%%%%%%%%%%%%%%%%%%%%%%%%%%%%%%%%%%%%%%%%%%
n1=1:2;
n2=3:4;
n3=5:6;

[b1,a1]=butter(5,.004);            %LPF 1
y(:,n1)=filter(b1,a1,Psd(:,n1)); %filters Channels 1 & 2 with LPF 1
[b2,a2]=butter(5,.001);            %LPF 2
y(:,n2)=filter(b2,a2,Psd(:,n2)); %filters Channels 3 & 4 with LPF 2
[b3,a3]=butter(5,.0005);           %LPF 3
y(:,n3)=filter(b3,a3,Psd(:,n3)); %filters Channels 5 & 6 with LPF 3

figure(1);
m=mean(y);  %returns a row vector with mean value in each column
pk=max(y);  %returns a row vector with max value in each column
snro=pk./m  %returns a row vector with SNR of each channel

for k=1:n,
   c(k)=1.8;                            %multiplier of mean
   if snro(k)>2;c(k)=snro(k)/1.112;end; %multiplier of mean
   z(:,k)=(sign(y(:,k)-c(k)*m(k))+1)/2; %determine threshold crossings
   aa(:,k)=diff(z(:,k));              %building the blocks of crossings
   len(k)=length(find(aa(:,k)));      %determine the number of blocks
```

```
    %%%%%%%%%%%%%%%%%%%%%%%%%%%%%%%%%%%%%%%%%%%%%%%%%%%%%%%%%%%%%%%%%%%%%%%%
    %%%                    Plots of deramped output                        %%%
    %%%%%%%%%%%%%%%%%%%%%%%%%%%%%%%%%%%%%%%%%%%%%%%%%%%%%%%%%%%%%%%%%%%%%%%%
    subplot(ceil(n/2),2,k)
    plot(f/1e6,y(:,k),f/1e6,.8*pk(k)*z(:,k));grid;
    axis([-fmax/1e6 fmax/1e6 0 1.2*pk(k)]);
    title([num2str(bws(k)/1e6),' MHz Deramp']);
    ylabel('Amplitude');

    %%%%%%%%%%%%%%%%%%%%%%%%%%%%%%%%%%%%%%%%%%%%%%%%%%%%%%%%%%%%%%%%%%%%%%%%
    %%%   Disqualifies Channels without effective deramped result   %%%
    %%%%%%%%%%%%%%%%%%%%%%%%%%%%%%%%%%%%%%%%%%%%%%%%%%%%%%%%%%%%%%%%%%%%%%%%
    if len(k)>4 ,
       count(k)=0; %Disqualifies if number of blocks greater than 2
    else
       L=find(aa(:,k));%determine location of threshold crossing blocks
       %%%%%%%%%%%%%%%%%%%%%%%%%%%%%%%%%%%%
       %determines the bandwidth of each block%
       %%%%%%%%%%%%%%%%%%%%%%%%%%%%%%%%%%%%
       w1(k)=1000*(L(2)-L(1));
       w2(k)= bws(k);
       if len(k)==4, w2(k)=1000*(L(4)-L(3)); end
       if w1(k)<0.25*bws(k) | w2(k)<0.25*bws(k),
          count(k)=1; %Accepted only blocks with sufficiently narrow
bandwidth
       else
          count(k)=0; %Blocks with wide bandwidth deemed to have no
deramp
       end
    end
end
xlabel('Frequency (MHz)');

channel=find(count);           %locate the useful channels
if isempty(channel)==1,        %no useful channels
   disp('No signal detected')
else
   [a,b]=max(snro(channel));  %useful channels with the best SNR
   disp(['FMCW detected in ',num2str(bws(channel(b))/1e6), ' MHz
Channel'])
end
```

B. DATA CAPTURING CODE (MATLAB CODE)

```
%  Program Name: capture_data.m
%  single-channel capture; A/D converter output
%  captures and transfers data from the CompuScope 2125 channel A to
vector sn

clear;clc;clf;

% set a system variable so that 'system' is defined in the first call
system.board(1).opmode = 1;

% find the CompuScope 2125 board and look for GAGESCOP.INC in the
Windows directory
boards_found = gagecall(0, 1, 0, system);

% if the board is not found, exit
if (boards_found < 1)
   error ('CompuScope board not found');
end

% set the system structure by calling setupcslpi.m
setupcslpi250;

% pass the system structure values to the DLL, which sets the hardware
accordingly
ret = gagecall(1, 0, 0, system);

if (ret == 1) % 1 is returned if the hardware set correctly
   disp('CompuScope 2125 hardware correctly set.');
end

if (ret <= 0) % negative numbers are returned when errors are detected
  error ('Errors in one or more capture parameters, program stopped');
end

% start capture - the DLL handles the trigger and busy timeouts
gagecall(2, 1, 1, system);

% convert the channel A samples to voltages and send them to MATLAB
sn = gagecall(3, 1, 0, system);

disp ('Data from channel A has been converted to voltages and sent to
MATLAB.');
disp ('The samples for channel A have been stored in the variable
(array) "sn".');

switch system.board.range_a
case 1   disp('A/D voltage range is +/- 5V')
case 2   disp('A/D voltage range is +/- 2V')
case 3   disp('A/D voltage range is +/- 1V')
case 4   disp('A/D voltage range is +/- 0.5V')
case 5   disp('A/D voltage range is +/- 0.2V')
case 6   disp('A/D voltage range is +/- 0.1V')
end
```

C. PARAMETER SETTING FOR THE COMPUSCOPE 2125 A/D CARD (MATLAB CODE)

```
% Program Name: setupcslpi.m
% Sets the board, capture, and channel structures for a single-channel
detector sample.

% Set the board structure
system.board.opmode = 1; % single-channel
system.board.sample_rate = 250e6; % 250 MHz sampling rate
system.board.range_a = 2; % 1 is +/- 5V, 2 is +/- 2V, 3 is +/- 1V
system.board.couple_a = 1; % DC coupling
system.board.source = 5; % software triggered
system.board.imped_a = 16; % 50 ohm
system.board.depth = 4194176; % fill the onboard RAM
% 4 megabytes (2e22) minus 128 bytes for trigger resolution

% Set the capture structure
system.capture.capture_type = 1; % normal capture (only available
option)
system.capture.trigger_timeout = 1000; % forced trigger after 10 msec
system.capture.busy_timeout = 65535; % abort capture after maximum
655.35 msec
system.capture.ensure_pre_trigger = 0; % do not ignore any triggers

% Set the channel structure
system.channel.enable = 1; % enables channel A
system.channel.start_point = 1048576; % discard first 10.5 msec of
samples
% (any transient response in the first 10.5 milliseconds will be
discarded)
system.channel.transfer_length = 250000; % 1 msec sample
```

D. OTHER MODE DETECTION RESULTS

1. Table of Summary for Results Enclosed

	Bandwidth of Transmitted LPI Signal	LPI Signal Strength	IF (MHz)	SNR (dB) Ch 1	Ch 2	Ch 3	Ch 4	Ch 5	Ch 6	Channel Selected
1.	1.5625 MHz	-105.60	82.20	**21.98**	15.90	10.84	8.99	5.95	4.22	1
2.	1.5625 MHz	-123.00	81.50	**7.79**	5.41	4.96	4.86	4.64	3.89	1
3.	1.5625 MHz	-125.50	82.31	5.75	5.61	4.98	5.03	4.64	3.84	no hit
4.	3.125 MHz	-112.30	83.91	6.04	**10.07**	5.20	5.18	4.72	3.86	2
5.	3.125 MHz	-115.70	83.81	5.66	**6.06**	5.01	5.01	4.65	3.83	2
6.	3.125 MHz	-115.20	83.81	5.44	**6.28**	5.01	4.99	4.69	3.72	2
7.	6.25 MHz	-110.30	83.29	6.17	6.68	**8.52**	5.02	4.56	3.92	3
8.	6.25 MHz	-113.50	83.73	5.78	5.89	**6.56**	5.37	4.79	3.79	3
9.	12.5 MHz	-88.90	82.25	13.03	12.97	13.33	**19.78**	11.13	6.82	4
10.	12.5MHz	-108.30	82.55	7.52	7.88	7.44	**12.60**	6.27	4.47	4
11.	12.5 MHz	-112.60	82.40	5.66	5.64	5.20	**7.02**	4.65	3.97	4
12.	25 MHz	-89.70	81.10	10.55	10.04	9.69	10.84	**14.85**	10.34	5
13.	25 MHz	-107.90	81.10	6.57	7.30	6.08	6.14	**8.79**	5.37	5
14.	50 MHz	-89.50	77.00	6.75	6.88	6.59	7.10	9.32	**14.56**	6
15.	50 MHz	-103.80	77.00	6.25	5.72	5.71	5.64	5.58	**8.23**	6
16.	50 MHz	-108.20	77.90	5.50	5.44	4.93	4.97	4.74	**6.06**	6
17.	2.5 MHz	-112.00	83.59	10.38	**10.70**	5.96	4.94	4.83	3.83	2
18.	5 MHz	-103.80	83.48	13.63	15.04	**16.24**	9.39	6.23	4.34	3
19.	30 MHz	-99.00	80.17	8.44	8.61	7.90	8.18	**12.93**	10.04	5
20.	40 MHz	-96.50	78.50	7.73	7.08	7.28	7.14	10.60	**12.48**	6
21.	No signal	-	-	5.77	5.84	5.21	5.07	4.76	3.78	no hit

Note: Bold font denotes maximum SNR channel.

	Transmitted Bandwidth	Signal Strength	IF (MHz)	Ch 1	Ch 2	Ch 3	Ch 4	Ch 5	Ch 6	Channel Selected
1.	1.5625 MHz	-105.60	82.20	**21.98**	15.90	10.84	8.99	5.95	4.22	1

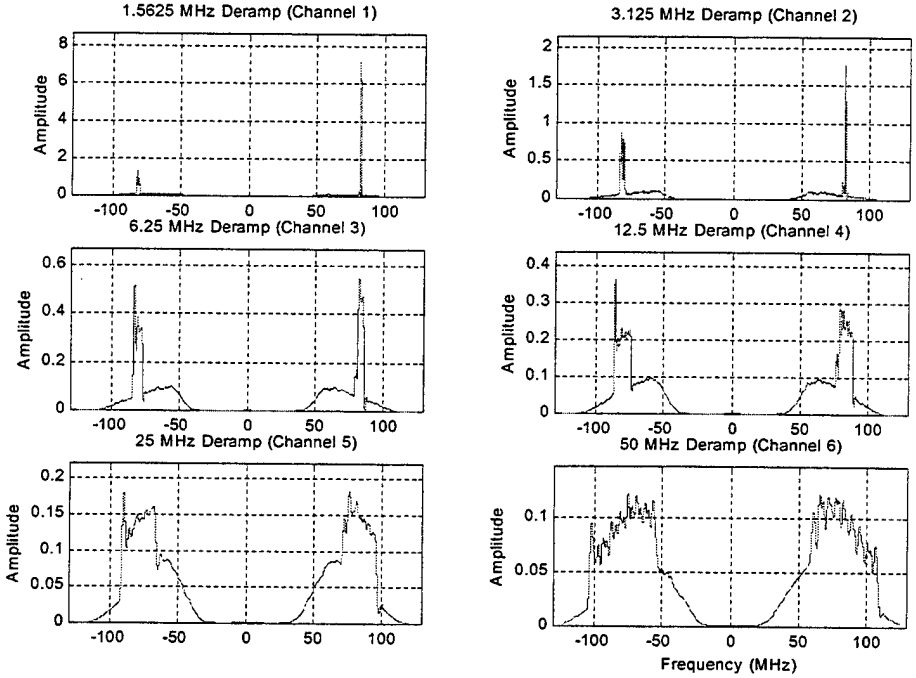

	Transmitted Bandwidth	Signal Strength	IF (MHz)	Ch 1	Ch 2	Ch 3	Ch 4	Ch 5	Ch 6	Channel Selected
2.	1.5625 MHz	-123.00	81.50	**7.79**	5.41	4.96	4.86	4.64	3.89	1

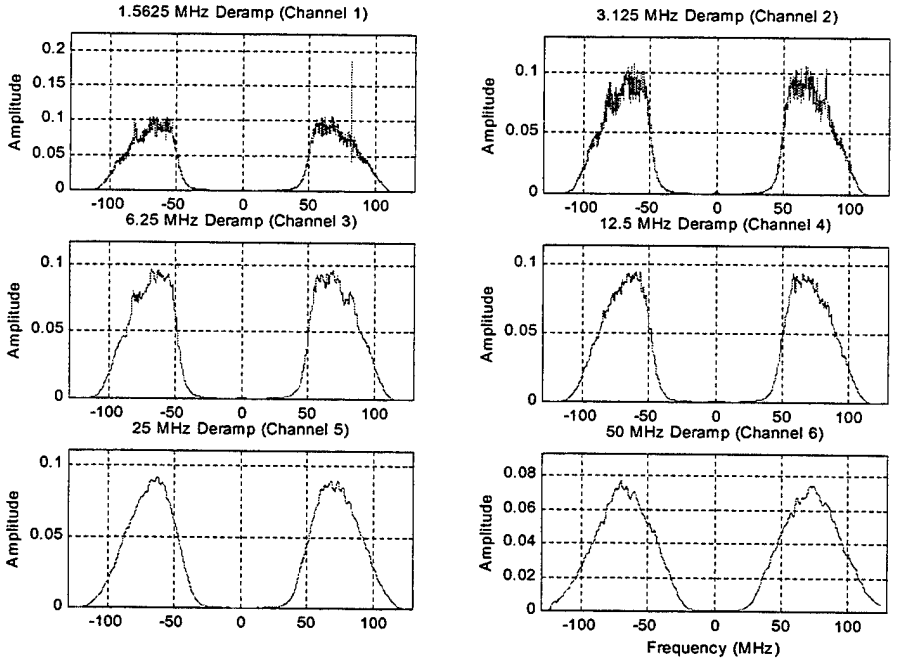

	Transmitted Bandwidth	Signal Strength	IF (MHz)	Ch 1	Ch 2	Ch 3	Ch 4	Ch 5	Ch 6	Channel Selected
3.	1.5625 MHz	-125.50	82.31	5.75	5.61	4.98	5.03	4.64	3.84	no hit

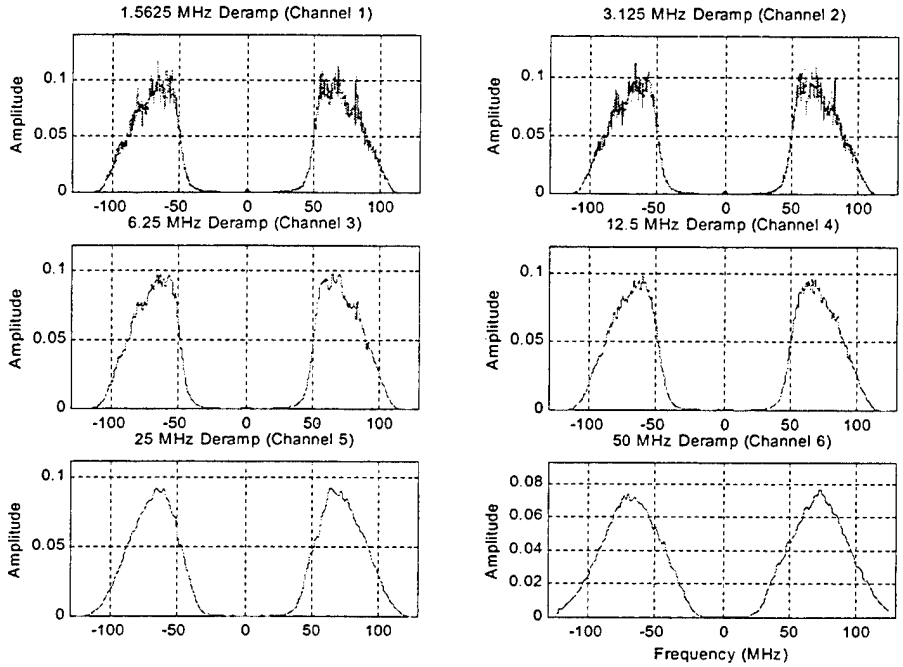

	Transmitted Bandwidth	Signal Strength	IF (MHz)	Ch 1	Ch 2	Ch 3	Ch 4	Ch 5	Ch 6	Channel Selected
4.	3.125 MHz	-112.30	83.91	6.04	**10.07**	5.20	5.18	4.72	3.86	2

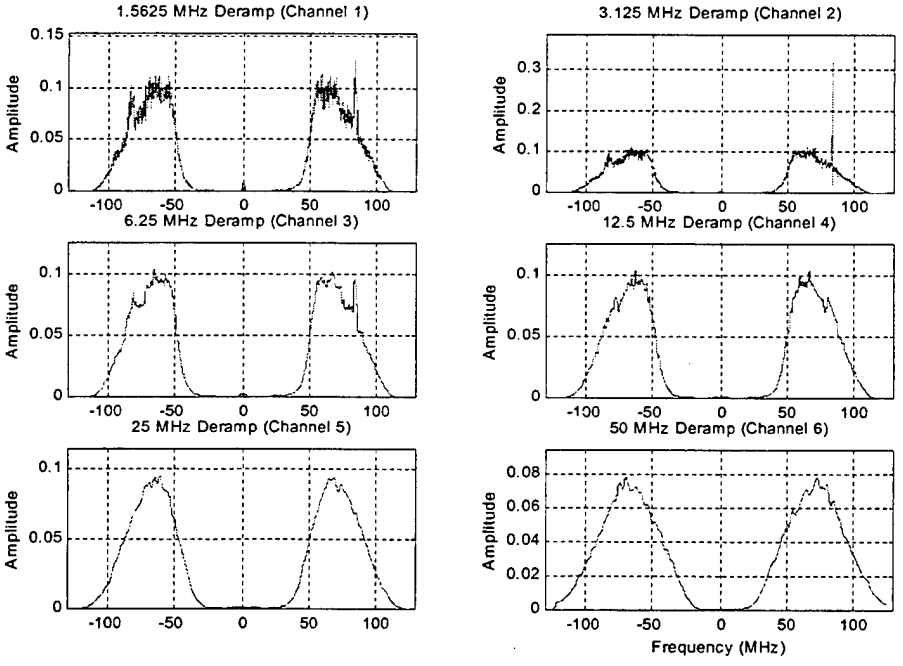

	Transmitted Bandwidth	Signal Strength	IF (MHz)	Ch 1	Ch 2	Ch 3	Ch 4	Ch 5	Ch 6	Channel Selected
5.	3.125 MHz	-115.70	83.81	5.66	**6.06**	5.01	5.01	4.65	3.83	2

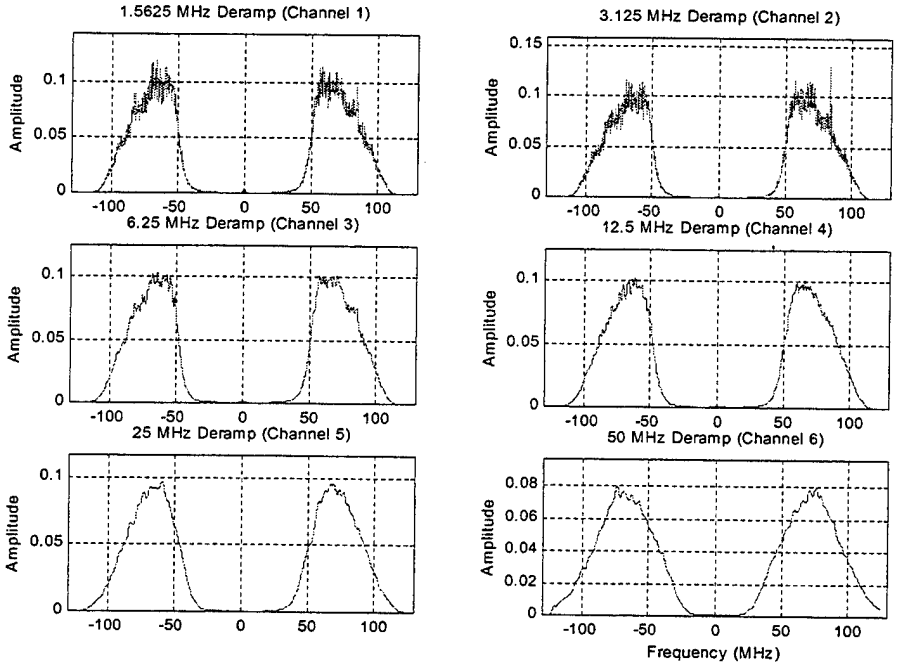

	Transmitted Bandwidth	Signal Strength	IF (MHz)	Ch 1	Ch 2	Ch 3	Ch 4	Ch 5	Ch 6	Channel Selected
6.	3.125 MHz	-115.20	83.81	5.44	**6.28**	5.01	4.99	4.69	3.72	2

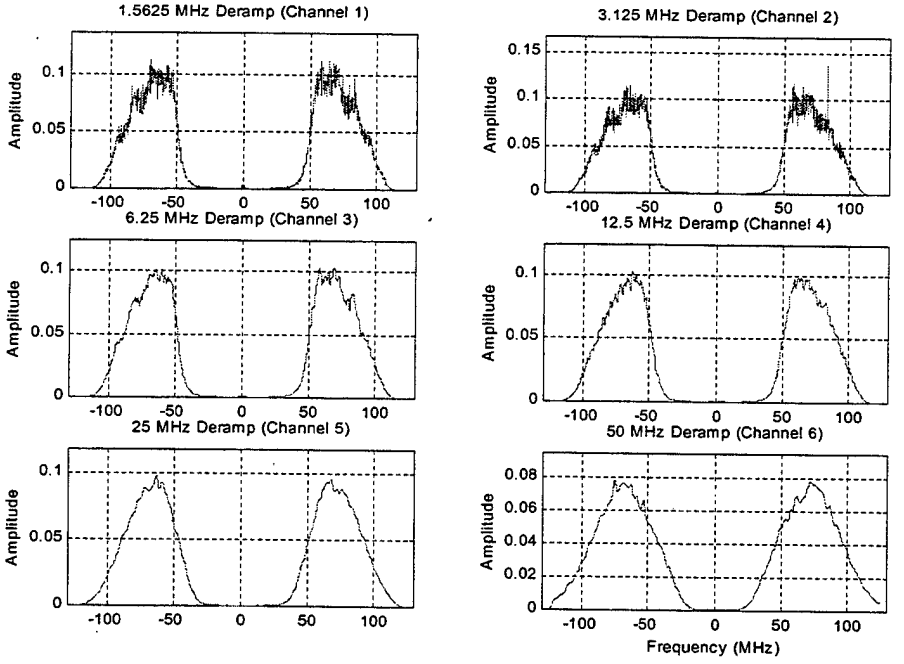

	Transmitted Bandwidth	Signal Strength	IF (MHz)	Ch 1	Ch 2	Ch 3	Ch 4	Ch 5	Ch 6	Channel Selected
7.	6.25 MHz	-110.30	83.29	6.17	6.68	**8.52**	5.02	4.56	3.92	3

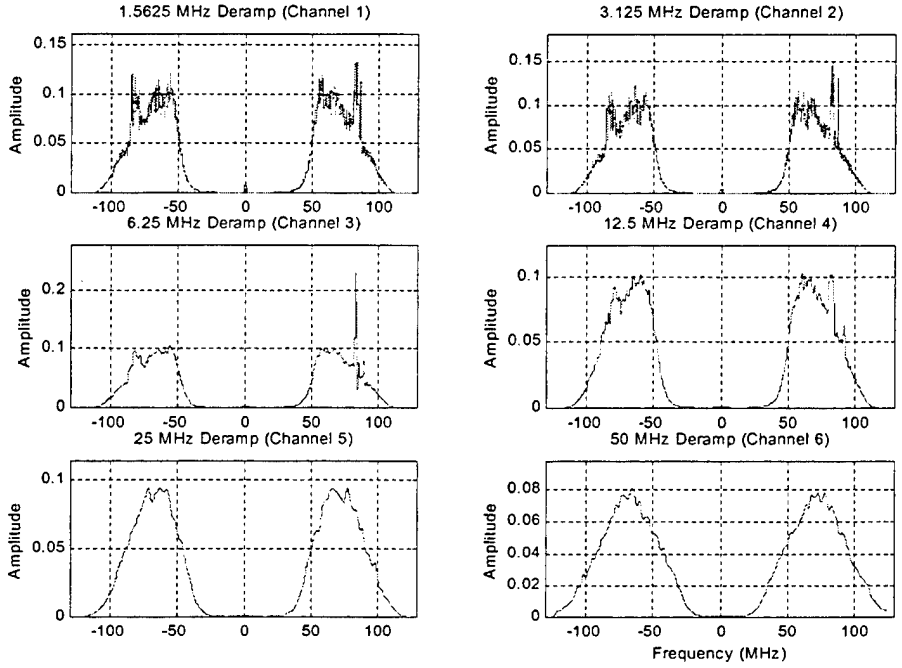

	Transmitted Bandwidth	Signal Strength	IF (MHz)	Ch 1	Ch 2	Ch 3	Ch 4	Ch 5	Ch 6	Channel Selected
8.	6.25 MHz	-113.50	83.73	5.78	5.89	**6.56**	5.37	4.79	3.79	3

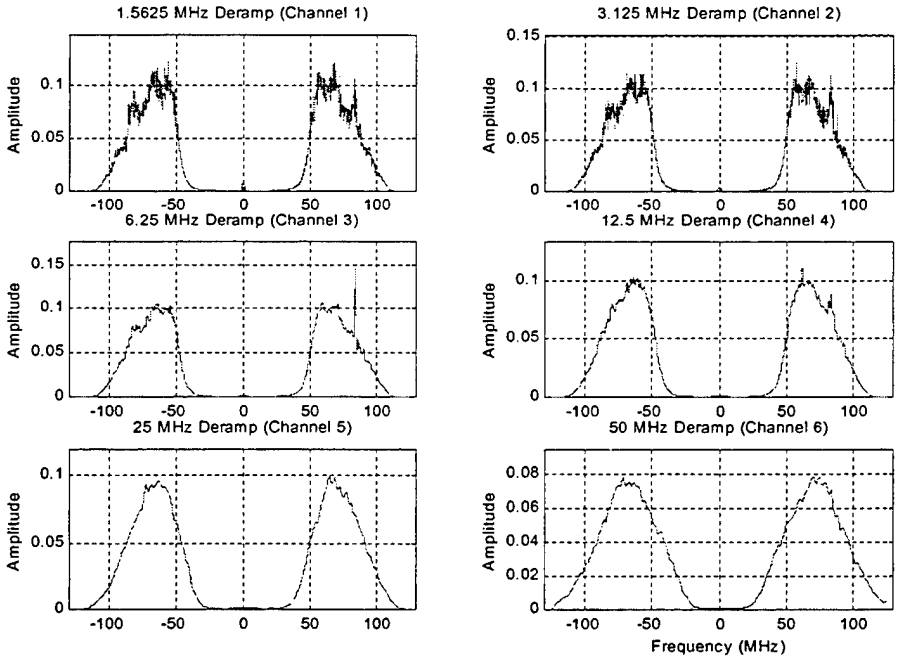

	Transmitted Bandwidth	Signal Strength	IF (MHz)	Ch 1	Ch 2	Ch 3	Ch 4	Ch 5	Ch 6	Channel Selected
9.	12.5 MHz	-88.90	82.25	13.03	12.97	13.33	**19.78**	11.13	6.82	4

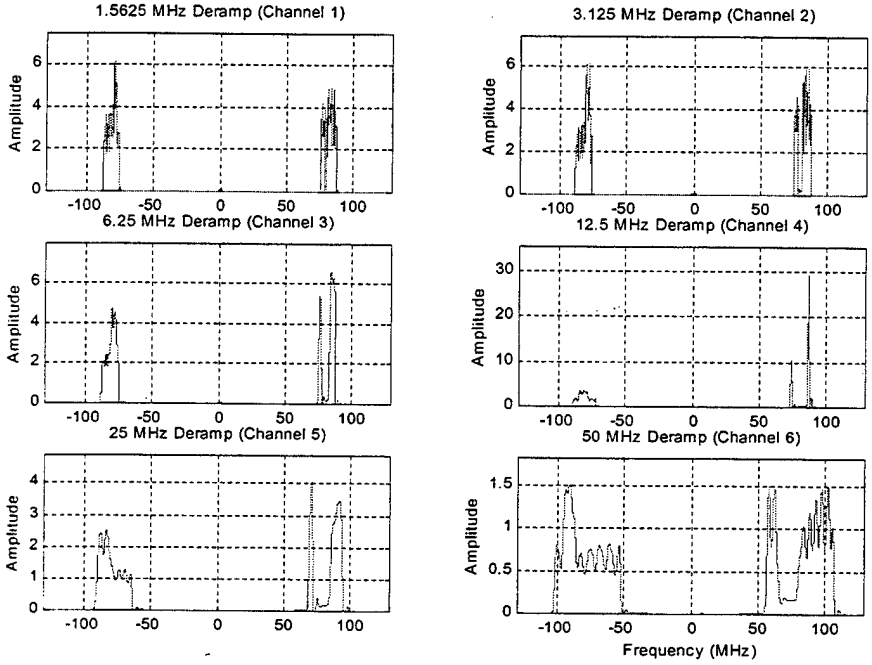

	Transmitted Bandwidth	Signal Strength	IF (MHz)	Ch 1	Ch 2	Ch 3	Ch 4	Ch 5	Ch 6	Channel Selected
10.	12.5MHz	-108.30	82.55	7.52	7.88	7.44	**12.60**	6.27	4.47	4

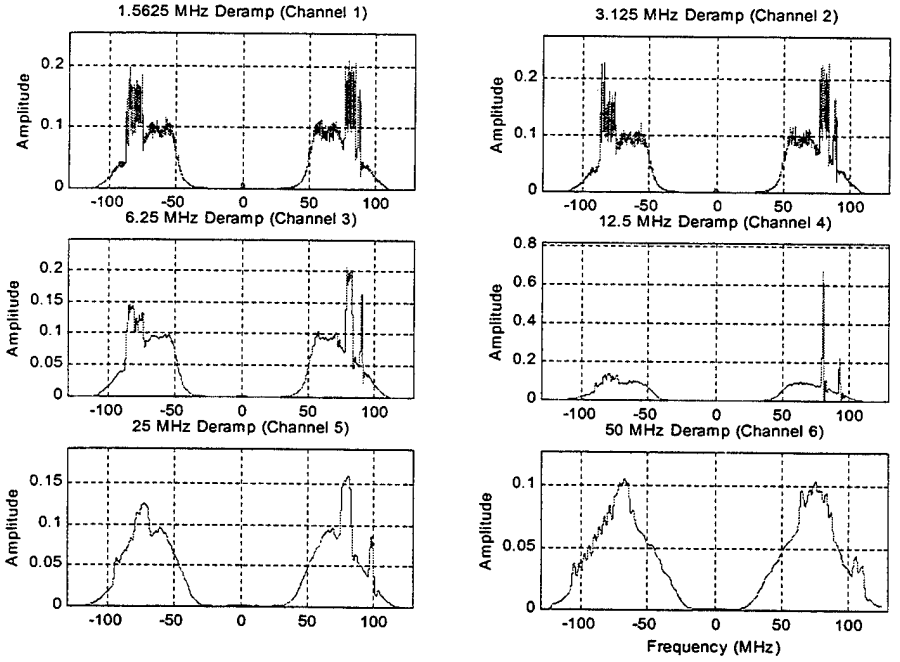

	Transmitted Bandwidth	Signal Strength	IF (MHz)	Ch 1	Ch 2	Ch 3	Ch 4	Ch 5	Ch 6	Channel Selected
11.	12.5 MHz	-112.60	82.40	5.66	5.64	5.20	**7.02**	4.65	3.97	4

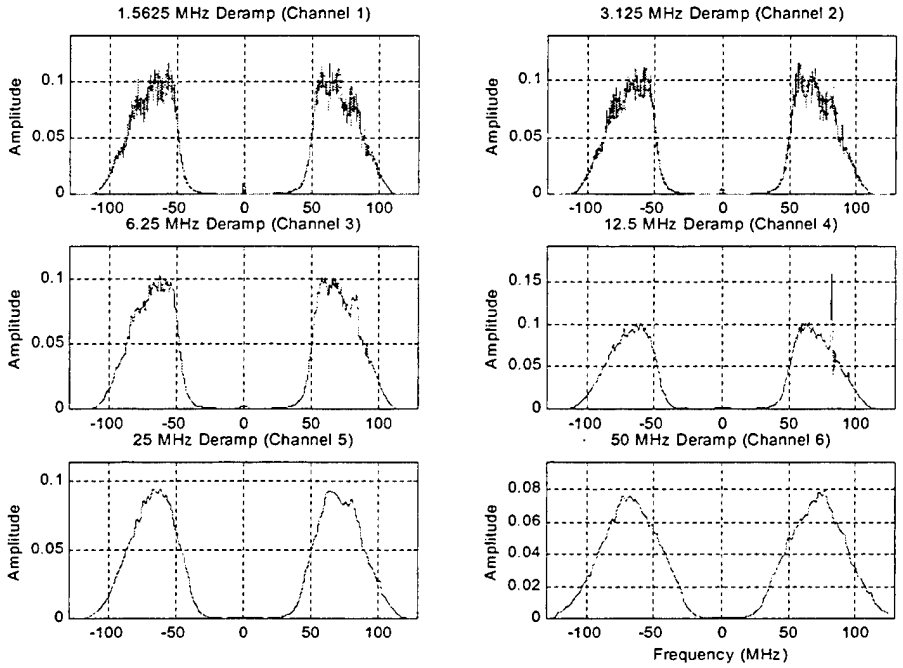

	Transmitted Bandwidth	Signal Strength	IF (MHz)	Ch 1	Ch 2	Ch 3	Ch 4	Ch 5	Ch 6	Channel Selected
12.	25 MHz	-89.70	81.10	10.55	10.04	9.69	10.84	**14.85**	10.34	5

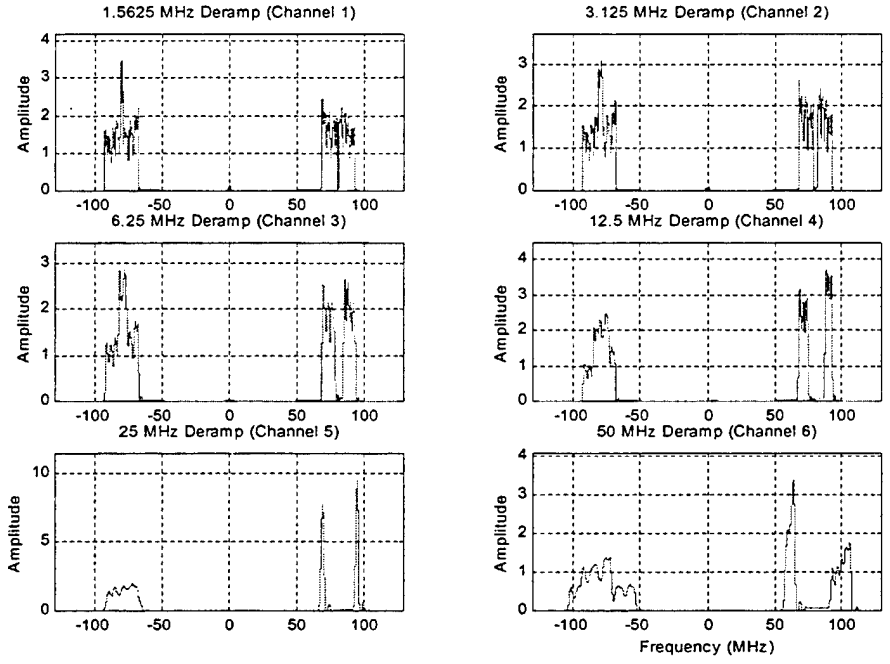

	Transmitted Bandwidth	Signal Strength	IF (MHz)	Ch 1	Ch 2	Ch 3	Ch 4	Ch 5	Ch 6	Channel Selected
13.	25 MHz	-107.90	81.10	6.57	7.30	6.08	6.14	**8.79**	5.37	5

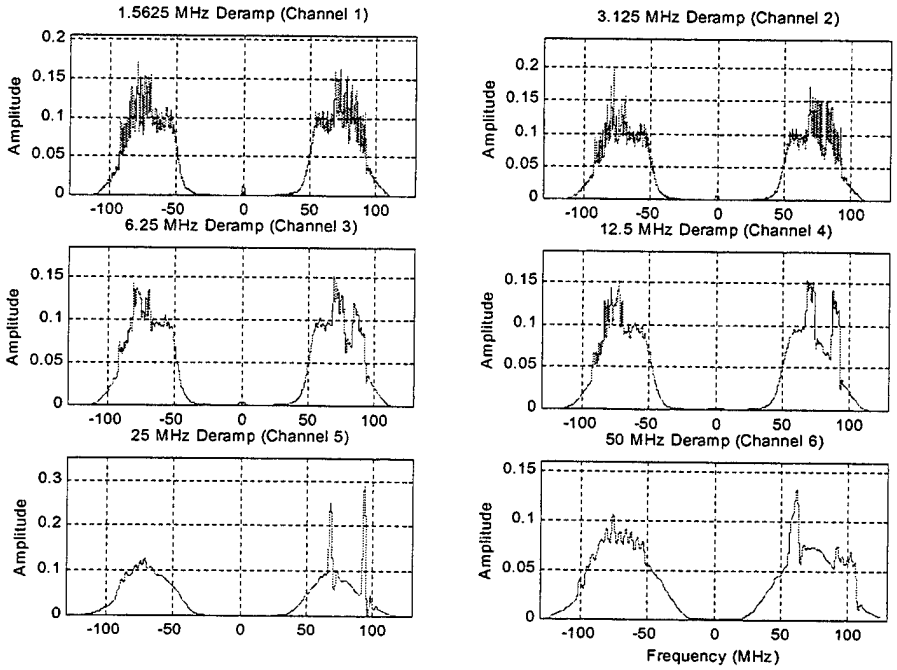

	Transmitted Bandwidth	Signal Strength	IF (MHz)	Ch 1	Ch 2	Ch 3	Ch 4	Ch 5	Ch 6	Channel Selected
14.	50 MHz	-89.50	77.00	6.75	6.88	6.59	7.10	9.32	**14.56**	6

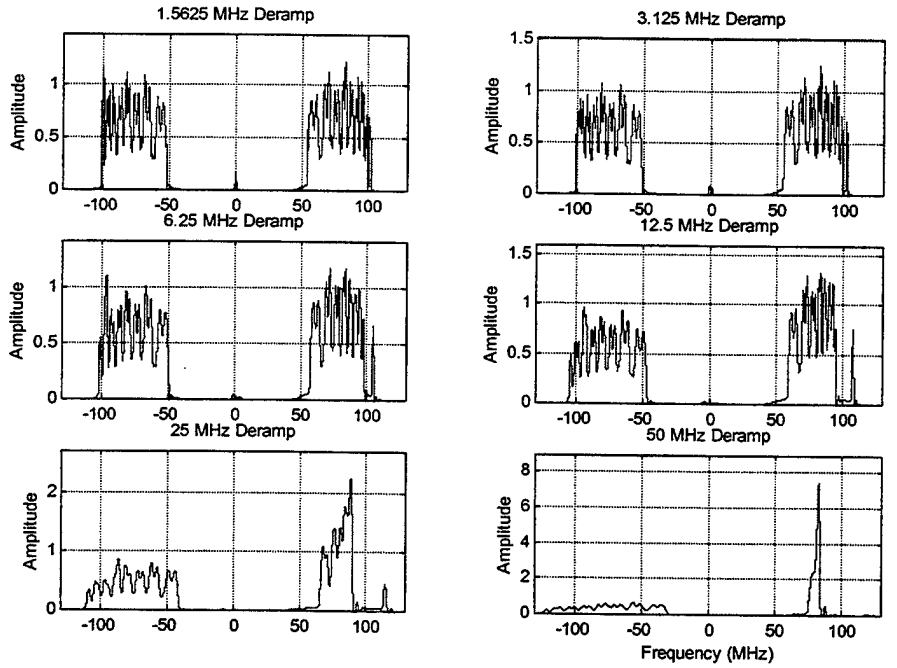

	Transmitted Bandwidth	Signal Strength	IF (MHz)	Ch 1	Ch 2	Ch 3	Ch 4	Ch 5	Ch 6	Channel Selected
15.	50 MHz	-103.80	77.00	6.25	5.72	5.71	5.64	5.58	**8.23**	6

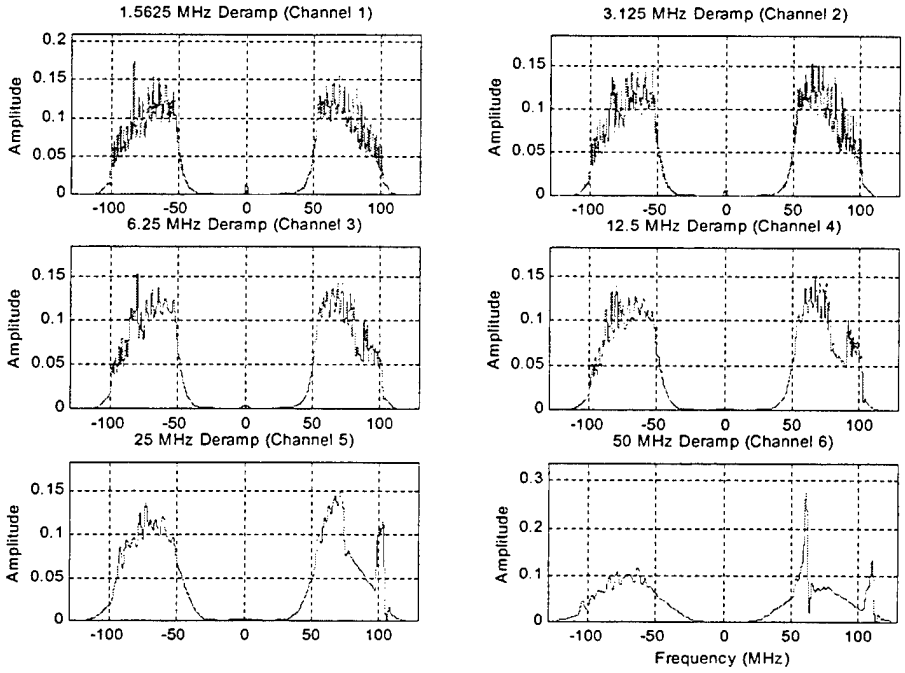

	Transmitted Bandwidth	Signal Strength	IF (MHz)	Ch 1	Ch 2	Ch 3	Ch 4	Ch 5	Ch 6	Channel Selected
16.	50 MHz	-108.20	77.90	5.50	5.44	4.93	4.97	4.74	**6.06**	6

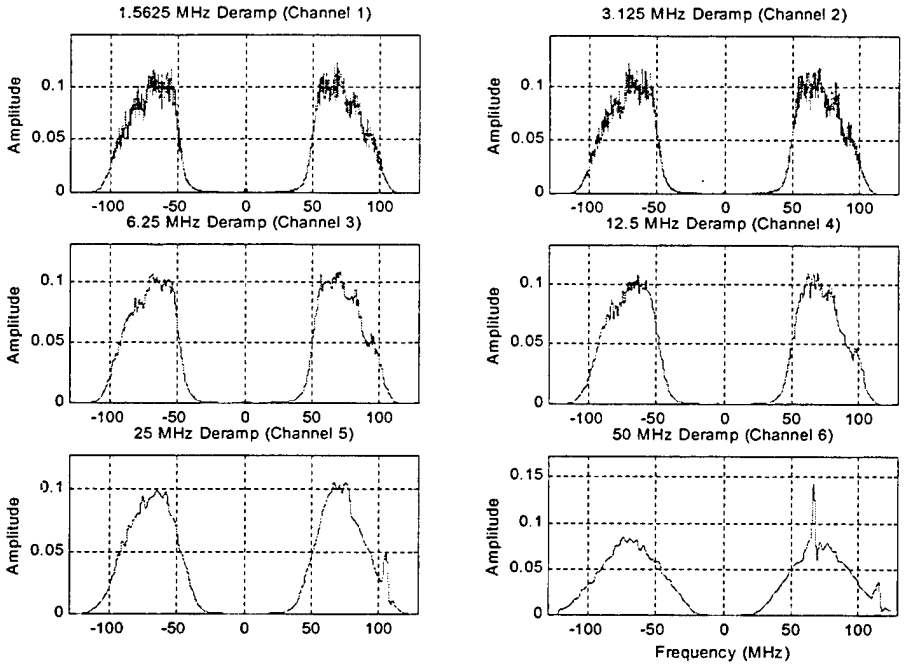

	Transmitted Bandwidth	Signal Strength	IF (MHz)	Ch 1	Ch 2	Ch 3	Ch 4	Ch 5	Ch 6	Channel Selected
17.	2.5 MHz	-112.00	83.59	10.38	**10.70**	5.96	4.94	4.83	3.83	2

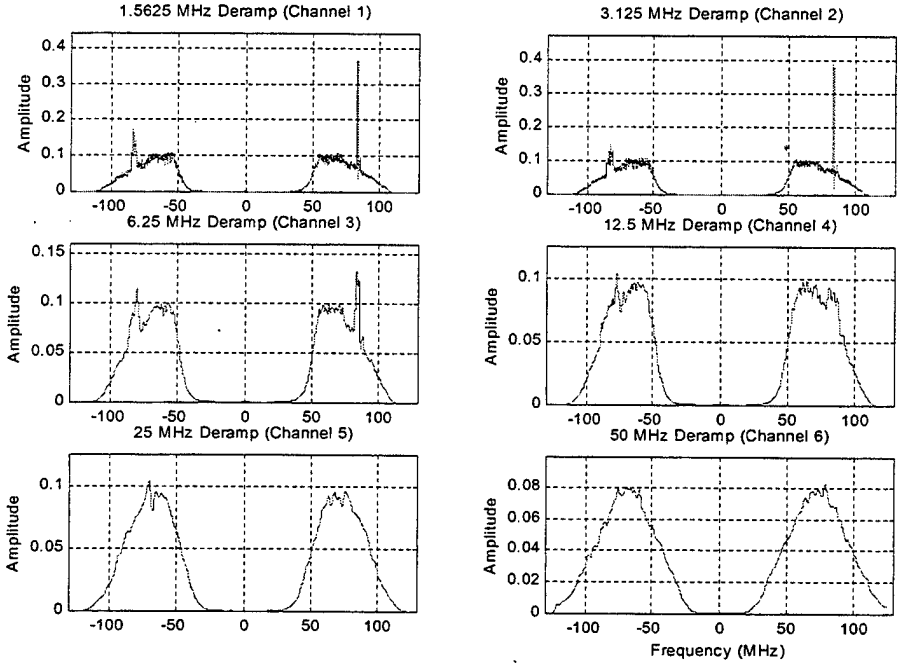

	Transmitted Bandwidth	Signal Strength	IF (MHz)	Ch 1	Ch 2	Ch 3	Ch 4	Ch 5	Ch 6	Channel Selected
18.	5 MHz	-103.80	83.48	13.63	15.04	**16.24**	9.39	6.23	4.34	3

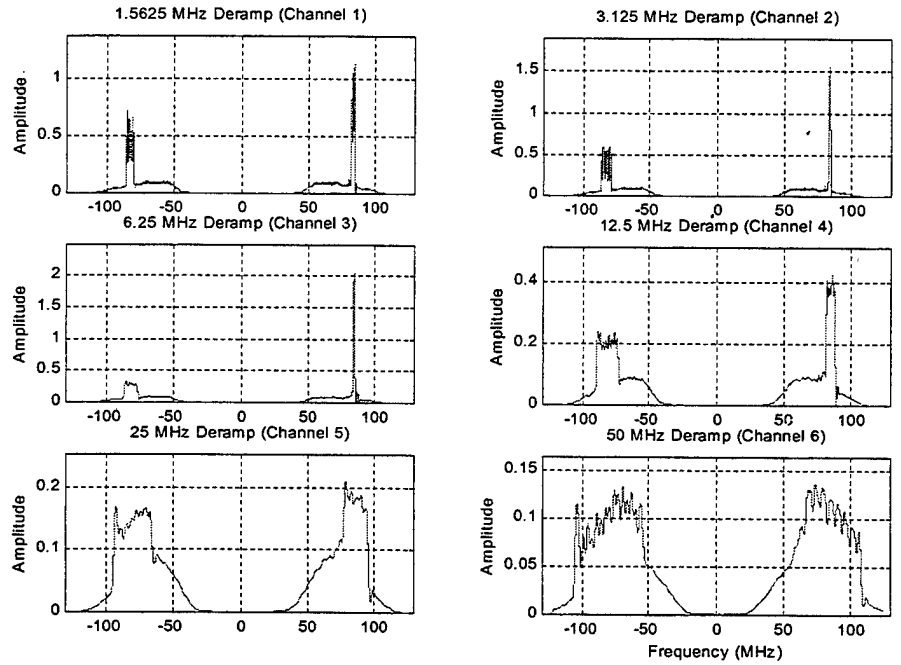

	Transmitted Bandwidth	Signal Strength	IF (MHz)	Ch 1	Ch 2	Ch 3	Ch 4	Ch 5	Ch 6	Channel Selected
19.	30 MHz	-99.00	80.17	8.44	8.61	7.90	8.18	**12.93**	10.04	5

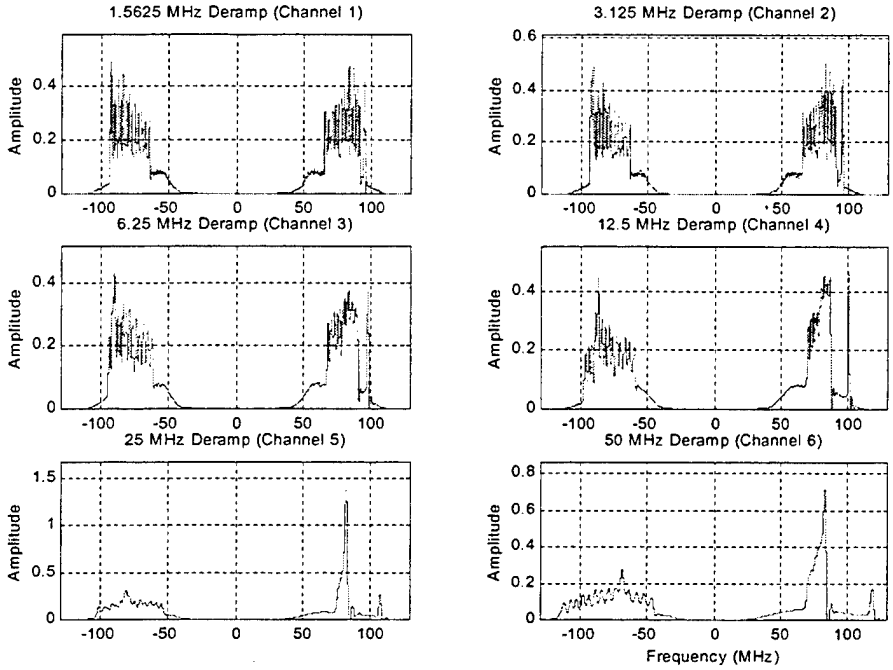

	Transmitted Bandwidth	Signal Strength	IF (MHz)	Ch 1	Ch 2	Ch 3	Ch 4	Ch 5	Ch 6	Channel Selected
20.	40 MHz	-96.50	78.50	7.73	7.08	7.28	7.14	10.60	**12.48**	6

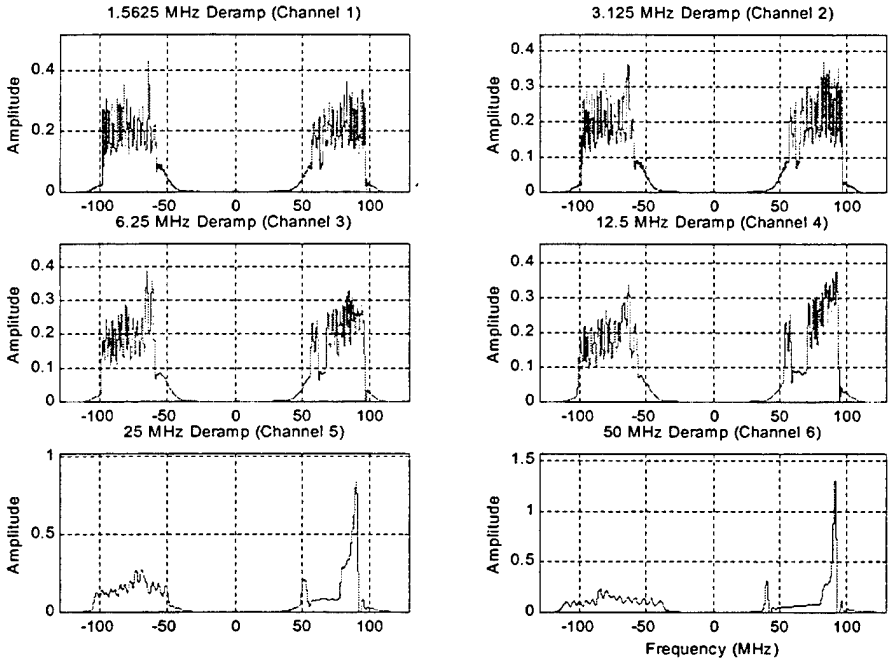

	Transmitted Bandwidth	Signal Strength	IF (MHz)	Ch 1	Ch 2	Ch 3	Ch 4	Ch 5	Ch 6	Channel Selected
21.	No signal (Noise only)	-	-	5.77	5.84	5.21	5.07	4.76	3.78	no hit

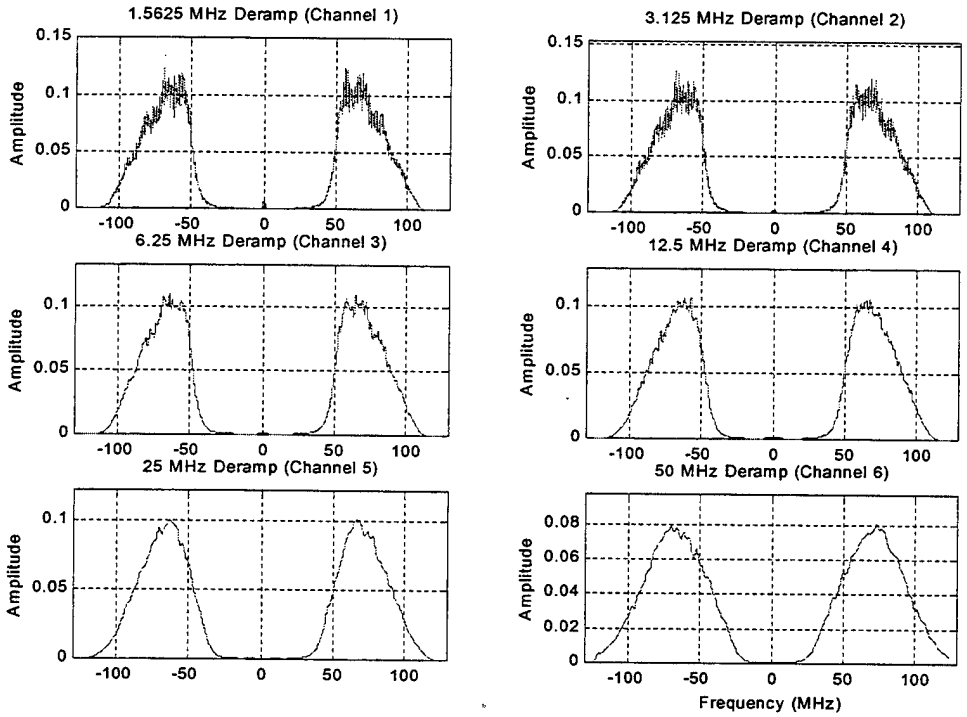

THIS PAGE INTENTIONALLY LEFT BLANK

INITIAL DISTRIBUTION LIST

1. Defense Technical Information Center 2
   8725 John J. Kingman Road, Suite 0944
   Ft. Belvoir, VA 22060-6218

2. Dudley Knox Library 2
   Naval Postgraduate School
   411 Dyer Road
   Monterey, CA 93943-5101

3. Prof Dan C. Boger 1
   Code IW
   Naval Postgraduate School,
   Monterey, CA93943-5101

4. Prof Curtis D. Schleher 1
   Code IW/Sc
   Naval Postgraduate School,
   Monterey, CA93943-5101

5. Prof David C. Jenn 1
   Code EC/Jn
   Naval Postgraduate School,
   Monterey, CA93943-5101

6. Prof Philip E. Pace 1
   Code EC/Pc
   Naval Postgraduate School,
   Monterey, CA93943-5101

7. Prof Herschel H. Loomis 1
   Code EC/Lm
   Naval Postgraduate School,
   Monterey, CA93943-5101

8. Maj Ong Peng Ghee 1
   27 Ellington Square
   Singapore 568938

9. Maj Teng Haw Kiad 1
   Block 627 Bukit Batok Central #13-646
   Singapore 650627